

CONTROL HEURISTICS FOR THE SOFT LANDING PROBLEM

by

Togay Tanyolaç

B.S., Mechanical Engineering, Boğaziçi University, 2008

Submitted to the Institute for Graduate Studies in
Science and Engineering in partial fulfillment of
the requirements for the degree of
Master of Science

Graduate Program in Industrial Engineering
Boğaziçi University
2013

CONTROL HEURISTICS FOR THE SOFT LANDING PROBLEM

APPROVED BY:

Assist. Prof. Hakan Yaşarcan
(Thesis Supervisor)

Prof. Yaman Barlas

Prof. Eşref Eşkinat

DATE OF APPROVAL: 22.01.2013

ACKNOWLEDGEMENTS

First of all, I would like to express my sincere gratitude to Assist. Prof. Hakan Yaşarcan, my thesis supervisor. His continuous effort in maintaining a seamless conversation and his attention to detail has taught me lessons both for scientific research and for life. Without his support and motivation it would be impossible to finish this work.

I am also thankful to Prof. Yaman Barlas, who introduced me to System Dynamics. I am sure he will remain a big inspiration to all of his students.

I would also like to thank Prof. Eşref Eşkinat for his valuable suggestions in improving this thesis.

Finally, I would like to extend my deepest gratitude to my family, especially to my parents Oya Tanyolaç and Haluk Tanyolaç. Without their understanding and endless support, any effort towards anything in life would be in vain. This is the most empowering thing I could ever hope for.

This research was supported by a Marie Curie International Reintegration Grant within the 7th European Community Framework Programme (grant agreement number: PIRG07-GA-2010-268272) and also by Bogazici University Research Fund (grant no: 5025-10A03P9).

ABSTRACT

CONTROL HEURISTICS FOR THE SOFT LANDING PROBLEM

In this thesis, we first construct a basic model representing the soft landing problem. The aim of the modeling effort is to transparently represent the process of landing a spacecraft on the surface of a celestial body. The process of landing is an interesting problem because there are two main contradictory performance criteria to be met simultaneously; the landing duration should be as short as possible, but at the same time crashing the spacecraft to the surface should be avoided. In this work, we studied four different control heuristics for the soft landing problem. The first heuristic is adapted from the mass-spring-damper model using the similarity of the equations of the soft landing model developed to the equations of the mass-spring-damper model. The second one is a bang-bang heuristic that first allows the spacecraft to fall freely, but after a critical point is reached, it uses the reverse force thruster at its maximum power until the touchdown. Bang-bang heuristic minimizes the time needed to land. The third heuristic is a combination of the bang-bang and mass-spring-damper heuristics. This new heuristic also borrows the concept *Weight of Supply Line* from System Dynamics literature. This new heuristic reconciles the two heuristics reducing their respective problematic behaviors. The last heuristic is the terminal guidance heuristic. The mass-spring-damper, bang-bang, new, and terminal guidance heuristics are compared in terms of their performances in the presence of an error in the parameter estimates, an error in the height readings, and an overlooked factor such as a delay in changing the level of the force created by the reverse force thruster, which is known as actuator delay. Terminal guidance heuristic and new heuristic lie in between mass-spring-damper heuristic and bang-bang heuristic in the sense that they require a more reasonable time to land as compared to the mass-spring-damper heuristic and they are not as sensitive as the bang-bang heuristic to the deviations from the original model. Finally, constant mass assumption is relaxed to observe a potential change in the behaviors generated by the heuristics, including the deviations due to errors and actuator delay. This relaxation also enables a comparison for the fuel consumption values of the heuristics.

ÖZET

YUMUŞAK İNİŞ PROBLEMİ İÇİN SEZGİSEL KONTROL YAKLAŞIMLARI

Bu tezde ilk önce yumuşak iniş problemini temsil eden bir model kuruyoruz. Modelleme çabasının amacı bir uzay aracının bir gökcismine inişini şeffaf bir şekilde temsil etmektir. İniş süreci ilginç bir problemdir çünkü iki karşıt performans ölçütü mevcuttur; iniş süresi mümkün olduğu kadar kısa olmalı, fakat aynı zamanda uzay aracının yüzeye çarpmasından da kaçınılmalıdır. Bu çalışmada, dört farklı sezgisel kontrol yaklaşımı inceledik. İlk sezgisel yaklaşım, yumuşak iniş modeliyle kütle-yay-sönüm modelinin denklemlerinin benzerliğinden yararlanılarak kütle-yay-sönüm modelinden uyarlandı. İkinci sezgisel yaklaşım ise önce uzay aracının serbestçe düşmesine izin veren, fakat bir kritik noktaya ulaştıktan sonra iticiyi iniş anına dek en yüksek güçte kullanan iki konumlu bir sezgisel yaklaşımdır. İki konumlu sezgisel yaklaşım, iniş süresini enküçükler. Üçüncü sezgisel yaklaşım, iki konumlu ve kütle-yay-sönüm sezgisel yaklaşımlarının bir kombinasyonudur. Ayrıca, bu yeni sezgisel yaklaşım Sistem Dinamiği literatüründen *Tedarik Hattı Ağırlığı* kavramını ödünç alır. Son sezgisel yaklaşım ise nihai kılavuz sezgisel yaklaşımıdır. Kütle-yay-sönüm, iki konumlu, yeni, ve nihai kılavuz sezgisel yaklaşımları performansları bakımından değişik durumlarda karşılaştırılmaktadırlar. Sözü edilen değişik durumlar; bir parametre ölçüm hatasının, yükseklik göstergelerinin okunmasında yapılan bir hatanın ve iticinin gücünün değiştirilmesinde tahrik düzeneği gecikmesi gibi bir etmenin gözden kaçırılmasının mevcudiyetidir. Nihai kılavuz sezgisel yaklaşımı ve yeni sezgisel yaklaşım, kütle-yay-sönüm yaklaşımına göre daha mantıklı bir iniş süresine ihtiyaç duymaktadırlar. Orijinal modelden sapmalara karşı ise iki konumlu sezgisel yaklaşıma göre daha dayanıklıdırlar. Dolayısıyla, nihai kılavuz yaklaşımı ve yeni sezgisel yaklaşım bu iki özellik açısından kütle-yay-sönüm ve iki konumlu sezgisel yaklaşımlarının arasındadırlar. Son olarak, sezgisel yaklaşımların davranışlarındaki potansiyel değişikliği gözlemlemek sabit kütle varsayımı gevşetilmiştir. Farklı sezgisel yaklaşımların yakıt sarfiyatlarının karşılaştırılmasını da mümkün kılan bu varsayım değişikliği, hataların ve tahrik düzeneği gecikmesinin mevcudiyetinde de incelenmiştir.

TABLE OF CONTENTS

ACKNOWLEDGEMENTS.....	iii
ABSTRACT.....	iv
ÖZET	v
LIST OF FIGURES	viii
LIST OF TABLES.....	xi
LIST OF SYMBOLS	xii
LIST OF ACRONYMS/ABBREVIATIONS.....	xiii
1. INTRODUCTION.....	1
2. THE STOCK MANAGEMENT STRUCTURE.....	6
3. THE SOFT LANDING MODEL.....	12
3.1. Selection of Landing Gear Parameters	16
3.2. Simplifying Model Assumptions	18
3.3. Performance Measures.....	19
4. A MASS-SPRING-DAMPER BASED CONTROL HEURISTIC.....	21
4.1. Selection of the Controller Parameters	24
4.2. Adjustments to the Mass-Spring-Damper Based Heuristic	25
4.3. Dynamic Behavior of Landing	26
5. BANG-BANG CONTROL HEURISTIC	31
6. A NEW HEURISTIC	35
7. TERMINAL GUIDANCE HEURISTIC FOR VERTICAL MOVEMENT.....	40
8. COMPARISON OF THE HEURISTICS AND THE SENSITIVITY OF THE HEURISTICS TO DEVIATIONS FROM THE MODEL ASSUMPTIONS	44
8.1. An Estimation Error in one of the Parameters	47
8.2. An Error in Height Readings	51
8.3. The Presence of an Actuator Delay	54
9. FUEL CONSUMPTION AND VARIABLE MASS	60
10. COMPARISON OF THE HEURISTICS UNDER VARIABLE MASS ASSUMPTION	62
11. CONCLUSION	65

APPENDIX A : CALCULATION OF THE CRITICAL POINT IN THE BANG-
BANG HEURISTIC..... 69
REFERENCES 70

LIST OF FIGURES

Figure 1.1.	Free body diagram of the vehicle with a control force (F) generated by the reverse force thruster and the gravitational force (GF).....	2
Figure 1.2.	The landing dynamics of Apollo 15.	3
Figure 2.1.	Stock management model with first order supply line.	9
Figure 3.1.	Stock-flow diagram of the model.	13
Figure 3.2.	Causal-loop diagram of the control feedback loop structure.....	14
Figure 3.3.	Maximum Landing Force variation with different Landing Velocity values displayed on five Suspension Damping Ratio Values.....	18
Figure 4.1.	Mass-spring-damper schematic.	21
Figure 4.2.	Landing Time and Absolute Landing Velocity variation with different Control Force Damping Ratios.	25
Figure 4.3.	Dynamic behavior of Height.....	28
Figure 4.4.	Dynamic behavior of Velocity.....	29
Figure 4.5.	Net force acting on the vehicle during landing.	29
Figure 4.6.	Absolute values of the forces acting on the vehicle during landing.	30
Figure 4.7.	Dynamic behavior of Spring Compression during the final process of landing (between seconds 55-60).	30
Figure 5.1.	Dynamic behavior of Height in the bang-bang heuristic.....	32

Figure 5.2.	Dynamic behavior of Velocity.....	33
Figure 5.3.	Net force acting on the vehicle during landing.....	34
Figure 5.4.	Absolute values of the forces acting on the vehicle during landing.	34
Figure 6.1.	Dynamic behavior of Height.....	38
Figure 6.2.	Dynamic behavior of Velocity.....	38
Figure 6.3.	Net force acting on the vehicle during landing.....	39
Figure 6.4.	Absolute values of the forces acting on the vehicle during landing.	39
Figure 7.1.	Dynamic behavior of Height in the terminal guidance heuristic.....	41
Figure 7.2.	Dynamic behavior of Velocity.....	42
Figure 7.3.	Net force acting on the vehicle during landing.....	42
Figure 7.4.	Absolute values of the forces acting on the vehicle during landing.	43
Figure 8.1.	Net Force profiles generated by the heuristics.....	45
Figure 8.2.	Landing behavior generated by the MSD heuristic in the presence of -50 kg error in the Mass estimate.....	49
Figure 8.3.	Landing behavior generated by the bang-bang heuristic in the presence of -50 kg error in the Mass estimate.....	49
Figure 8.4.	Landing behavior generated by the new heuristic in the presence of - 50 kg error in the Mass estimate.....	50
Figure 8.5.	Landing behavior generated by the terminal guidance heuristic in the presence of -50 kg error in the Mass estimate.....	50

Figure 8.6.	Landing behavior generated by the MSD heuristic in the presence of +10 m error in Height reading.	52
Figure 8.7.	Landing behavior generated by the bang-bang heuristic in the presence of +10 m error in Height reading.	53
Figure 8.8.	Landing behavior generated by the new heuristic in the presence of +10 m error in Height reading.	53
Figure 8.9.	Landing behavior generated by the terminal guidance heuristic in the presence of +10 m error in Height reading.	54
Figure 8.10.	Responses of different order delay structures to a step input.	55
Figure 8.11.	Landing behavior generated by the MSD heuristic in the presence of discrete actuator delay.	57
Figure 8.12.	Landing behavior generated by the bang-bang heuristic in the presence of discrete actuator delay.	57
Figure 8.13.	Landing behavior generated by the new heuristic in the presence of discrete actuator delay.	58
Figure 8.14.	Landing behavior generated by the terminal guidance heuristic in the presence of discrete actuator delay.	58
Figure 8.15.	Velocity profiles of the new heuristic with different orders of delay.	59
Figure 8.16.	Landing behavior generated by the new heuristic in the presence of a second order delay of 2 seconds.	59
Figure 10.1.	Force utilization of the bang-bang heuristic when mass decays due to fuel consumption.....	63

LIST OF TABLES

Table 3.1.	Comparison of sample landing velocities and corresponding SDR values minimizing maximum force subjected to the landing gear.	17
Table 8.1.	Comparison of the four heuristics.....	44
Table 8.2.	Comparison of the landing performances of the heuristics in the existence of an error in the parameter estimate <i>Mass</i>	48
Table 8.3.	Comparison of the landing performances of the heuristics in the existence of an error in the variable reading <i>Height</i>	52
Table 8.4.	Comparison of the landing performances of the heuristics in the existence of a 2 second actuator delay.....	55
Table 10.1.	Comparison of the landing performances of the heuristics with variable mass.....	64

LIST OF SYMBOLS

a	Acceleration
c	Velocity Coefficient
F	Control Force
F^*	Desired Net Force
F_{damper}	Damper Force
F_{external}	External Force
F_{net}	Net Force
F_{spring}	Spring Force
g_0	Earth Gravitational Acceleration
H	Height
I_{sp}	Specific Impulse
k	Height Coefficient
m	Mass
S	Stock
S^*	Desired Stock
v	Velocity
w_{SL}	Weight of Supply Line
x	Distance

LIST OF ACRONYMS/ABBREVIATIONS

ADT	Acquisition Delay Time
AF	Acquisition Flow
CF	Control Flow
GF	Gravitational Force
LF	Loss Flow
SA	Stock Adjustment
SAT	Stock Adjustment Time
SDR	Suspension Damping Ratio
SL	Supply Line
SL*	Desired Supply Line
SLA	Supply Line Adjustment

1. INTRODUCTION

Soft landing is an interesting and challenging problem in space exploration. The process of landing is a challenging task because there are two main contradictory performance criteria to be met simultaneously; the landing duration should be as short as possible, but at the same time crashing the spacecraft to the surface should be avoided (Liu, Duan, and Teo, 2008). In order to achieve a fast and safe landing on the surface of a celestial body, the landing process should be controlled. When landing on celestial bodies with no atmosphere (e.g. the moon), deceleration strategies that rely on the drag force (e.g. a parachute) do not work due to the absence of atmospheric molecules. Therefore, a reverse force thruster, which will decelerate the vehicle, is needed (see Figure 1.1). The design of reverse force thrusters for spacecrafts first came into focus during the establishment of the space programs of the Soviet Union and USA (Rosen, Schwenk 1959). Manned lunar discovery projects set on with the landing of Apollo 11 on the moon in 1969 and peaked in the 1970s. The last manned vehicle on the moon was in 1972. However, the interest on landing on the moon continues with current and future unmanned projects from several countries (USA, China, South Korea, Japan, Russia, India, Iran, UK, EU). The design interest in lunar vehicles and their descent stages is not lost. Human return to the moon is planned for the exploration of further destinations including Mars among others (Wu *et al.* 2007).

Guidance algorithms for the navigation and the descent on the moon have been studied. Linear and quadratic second-order differential equations (Klumpp, 1974; Kriegsman and Reiss, 1962) controlling the descent have been proposed among others. It is worth mentioning that the algorithm proposed by Klumpp has been used by NASA in the six manned lunar landings and, later, published in 1974.

Fuel optimal landing strategies have also been studied early on during the space program by government related agencies and later by scientists in the field, revealing that the minimum time problem is equivalent to the minimum fuel problem. These past studies revealed bang-bang control solutions. (Meditch, 1964; Flemming and Rishel, 1975; Cantoni and Finzi, 1980).

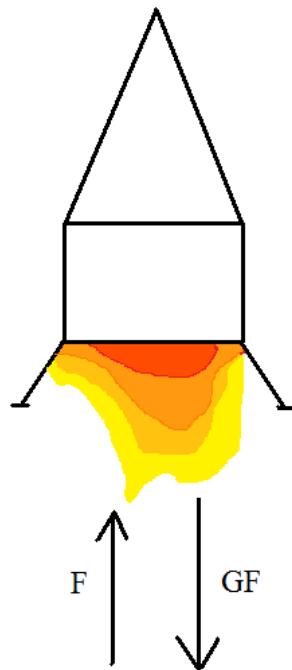


Figure 1.1. Free body diagram of the vehicle with a control force (F) generated by the reverse force thruster and the gravitational force (GF).

A reasonable landing process requires a control heuristic that will ensure the safety of the spacecraft, which practically means a soft touchdown of the spacecraft to the surface of the celestial body at the end of the landing process. Note that the landing force (the force created at the time of touchdown) is a complex result of the landing velocity (the velocity with which the spacecraft touches the surface), the landing gear parameters of the spacecraft, the mass of the spacecraft, and the gravitational force. Out of these four important components that determine the landing force, a control heuristic can only have an effect on the landing velocity. Moreover, this effect is indirect. Control heuristic determines the control force, control force results in the net force, net force determines the acceleration, acceleration gradually adjusts the velocity, and the value of velocity at the time of touchdown becomes the landing velocity. Therefore, it is not an easy task to manage the landing velocity at around a desired level. Moreover, the heuristic that will be employed should also manage the length of the time needed to land at a reasonably low value because a long landing duration requires extensive fuel usage. The two criteria, minimizing the landing velocity and minimizing the length of the time needed to land, are contradictory, which makes the soft landing problem a challenging task. A control heuristic

aiming to satisfy the two criteria, should allow the vehicle descend to the surface rather quickly, but make it decelerate safely to low velocity values before the instant of landing (Liu, Duan, and Teo, 2008; Zhou *et al.*, 2009). The landing dynamics of Apollo 15 is an example of this strategy (Figure 1.2).

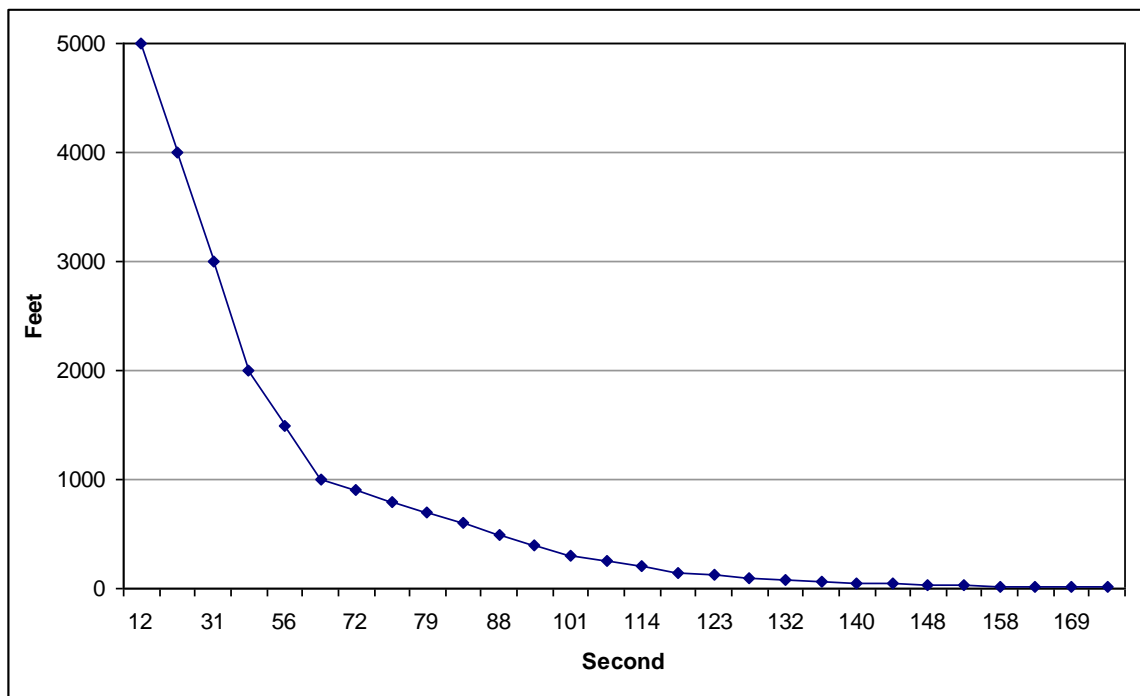


Figure 1.2. The landing dynamics of Apollo 15.

In plotting the dynamics observed in Figure 1.2, we connected to the Apollo 15 entry of the Wikipedia website (http://en.wikipedia.org/wiki/Apollo_15; accessed on 16 September 2011) and time coded the landing video on the page (http://en.wikipedia.org/wiki/File:Apollo_15_landing_on_the_Moon.ogg; accessed on 16 September 2011). Note that, Apollo 15 was the fourth of the six manned vehicles to land on the Moon (30 July 1971).

In this thesis work, we first construct a basic model representing the soft landing problem. The aim of the modeling effort is to transparently represent the process of landing a spacecraft on the surface of a celestial body. We modeled the soft landing challenge using System Dynamics (SD) simulation methodology because SD has a strong focus on the explicit representation of the problem related elements of a system (Barlas, 2002; Forrester, 1961; Forrester, 1971; Sterman, 2000). The SD methodology is briefly presented

in Chapter 2, with the inclusion of the stock-flow diagram and the equations for the generic stock management structure. The model and its assumptions are presented in Chapter 3. Many real life complexities such as delays caused by actuators and measurement processes are not represented in the model. Even under the simplifying model assumptions, the main goal of the soft landing problem still remains a challenging one because the two state variables “height” and “velocity” can only be indirectly controlled.

In Chapter 4, we present a control heuristic (i.e. control law) adapted from the mass-spring-damper model. The mass-spring-damper based control heuristic is adapted from the mass-spring-damper model using the similarity of the equations of the soft landing model given in Chapter 3 to the equations of the mass-spring-damper model; both models can be reduced to a second order linear differential equation. The behavior obtained from the mass-spring-damper based control heuristic is discussed in detail in Chapter 4.

The bang-bang heuristic dynamically calculates a critical point. It first allows the spacecraft to fall freely, but after the critical point is reached, it uses the reverse force thruster at its maximum power until the touchdown (Meditch, 1964). The bang-bang heuristic and the corresponding landing dynamics are discussed in Chapter 5.

In Chapter 6, a new heuristic is developed combining elements from the bang-bang heuristic and the mass-spring-damper heuristic. Additionally, this new heuristic includes the weight of supply line concept used in the anchor-and-adjust heuristic, which is widely used in stock management. In Chapter 2, anchor-and-adjust heuristic is presented together with the generic stock management structure. Although, this new heuristic is not superior to the bang-bang heuristic and the mass-spring-damper heuristic in every aspect, it succeeds in improving their most problematic responses. Note that, both the mass-spring-damper heuristic and the anchor-and-adjust heuristic are in essence proportional derivative feedback control applications.

In Chapter 7, a heuristic adapted from Kriegsman and Reiss (1962), terminal guidance heuristic, is presented. The core of the formulation of this heuristic is the ratio of the square of the velocity to the height. This ratio is used to calculate command

acceleration for the vehicle and the command acceleration is used to obtain the control force.

The mass-spring-damper heuristic, the bang-bang heuristic, the new heuristic, and the terminal guidance heuristic have different characteristics. The resulting behaviors of the four heuristics are compared in Chapter 8. The strengths and weaknesses of the heuristics are also discussed in Chapter 8 using three different types of deviations from assumptions (an error in the parameter estimates; an error in the state variable readings; a delay in changing the level of the force created by the reverse force thruster, which is known as actuator delay), each containing four scenarios.

In Chapter 9, the constant mass assumption is relaxed. A variable mass is defined based on fuel consumption, which is calculated depending on the value of the used force. Some equations given in Chapter 3 are modified to reflect this assumption change.

The comparison of the behaviors of the four heuristics under the variable mass assumption, with the same three types of deviations discussed in Chapter 8, is done in Chapter 10. The differences between the performances of the models with and without constant mass assumption are also discussed in Chapter 10.

2. THE STOCK MANAGEMENT STRUCTURE

System Dynamics is an interdisciplinary methodology for modeling and understanding how complex systems change over time (Barlas, 2002; Barlas and Yasarcan, 2006; Forrester, 1961; Forrester, 1971; Sterman, 2000). Stock Management is one of the important and well-studied problems in System Dynamics (Yasarcan and Barlas, 2005; Yasarcan, 2010). Main modeling objects are stocks and flows¹ in System Dynamics. “Stocks are accumulations ... Stocks are altered by inflows and outflows” (Sterman, 2000, p. 192). Stocks characterize the state of the system; they give systems inertia and memory. A flow or flows attached to a stock, however, describe the way the stock changes over time (Barlas, 2002; Forrester, 1971; Sterman, 2000). A stock is usually managed via controlling one of its flows. Usually, this flow is its inflow (Sterman, 2000; Yasarcan and Barlas, 2005; Yasarcan, 2010).

Stock management is the task of controlling stocks through the appropriate selection of time and level of the decision flows (Maynard, 1971). This control flow, in this case either inflow to or outflow from the stock, represents the actions resulting from the decisions that we make. These decisions are generated by dynamic decision-making heuristics aiming to close the discrepancy between the stock and its desired level. Usually, a deviation from the desired state has associated costs or penalty (Sterman, 1989). In addition to the discrepancy between the stock and its desired level, there are other inputs to the decision making process. Ideally, the decision maker should also consider the loss flow in his decisions and try to compensate for it while deciding on the amount of the control he applies. Moreover, it takes time for the decisions to affect the stock that we manage in realistic cases. This time difference between the control actions and their effects complicate the task of stock management (Sterman, 2000, Chapter 17).

Inventory Management is an example of the generic stock management problem. Inventory is the main stock of an inventory management system and its level is changed via its flows; shipments and arrivals of goods. Shipments, which is driven by the sales, is

¹ Stocks are represented as boxes and flows are represented as arrows attached to these boxes.

the outflow from the inventory. Arrivals of goods, which is the delayed version of our orders, is the inflow to the inventory. In production systems, this delay is caused by the production process. In a supply chain, this delay would be the in-transit time between our orders to our suppliers and arrival of goods. The presence of the delay between orders and arrivals makes it difficult to maintain the inventory at its desired level. As a result, the level of the inventory subject to control would usually show oscillatory behavior. Such behavior is unwanted because that would mean overstocking and backlog from time to time, which are both costly (Barlas and Ozevin, 2004; Yasarcan, 2010).

Glucose-insulin regulatory system can also be modeled as a stock management problem. The blood glucose concentration level, which is the main stock of this system, needs to be maintained within certain limits. As glucose concentration is a stock, the change in its level depends on its flows. The inflows are glucose intake through digestion and hepatic glucose production; the outflow is glucose utilization. Blood insulin concentration level has a strong effect on glucose utilization. In a healthy person's body, blood glucose concentration is regulated within certain limits via regulating blood insulin concentration, which is another important stock of the glucose-insulin regulatory system. In patients with Diabetes Mellitus Type I, insulin cannot be produced sufficiently in the pancreas, which leaves glucose unregulated. Therefore, these patients must control their blood glucose concentration levels manually with insulin shots, typically after having a meal. There are delays involved in the glucose-insulin regulatory system, which make it difficult to maintain the concentrations of glucose and insulin within their desired ranges. Therefore, the appropriate dosage and time of the insulin injection is difficult to determine. Late or low insulin admission may cause a hyperglycemic state (excessive blood glucose level), which is harmful to many organs, especially liver and the eyes. Early or high insulin admission may end up in a hypoglycemic state (insufficient blood glucose level), which may lead to impaired brain function, unconsciousness, and even death (Herdem and Yasarcan, 2010).

Managing the fullness level at the dinner table is also a stock management problem. There is a desired level of fullness; the states of being hungry and being overfilled are unwanted. Eating is the inflow to the fullness level and the outflow is the digestion. The fullness level is not perceived instantaneously as soon as a bite is swallowed. There is a

time difference between eating and the perception of its contribution to the fullness level. Due to this delay, one could carry on eating, although the currently taken food would suffice. This would cause an overshoot of the ideal fullness level, which may create discomfort.

As mentioned in the previous paragraphs, there usually is a time difference between a control action and its effect on the main stock. The total amount of control actions yet to affect the main stock is called “supply line”. In the inventory management example given earlier, the supply line would be the goods in transit and the supply line delay would be the in transit time. In a workforce management system, the main stock would be the workforce level, the supply line would be the new recruits undergoing their training period, and the supply line delay time would be the duration of the training. In a production system, the main stock would be the finished goods inventory, the supply line would be the work-in-process inventory, and the supply line delay time would be the duration of the production process. There are many factors that should be considered in the decision making process such as the level of the main stock and the expected rate of the outflow. The level of the supply line should also be considered in the decisions. Otherwise, depending on the values of the decision making parameters, the main stock would either show an unwanted oscillatory behavior or a poor response (i.e. the gap between the main stock and its ideal level would reduce undesirably slowly). In system dynamics, mainly, there are three types of delay structures. The supply line examples given in this paragraph are all in the form of a material supply line delay. Stock management in the presence of such a delay structure is well-studied and there exists dynamic decision making heuristics that can prevent the unwanted behaviors mentioned before (Sterman, 1989; Sterman, 2000, Chapter 17; Yasarcan, 2003, Chapter 5; Yasarcan, 2011).

The figure below is the stock-flow diagram of the generic stock management structure with a first order supply line delay.

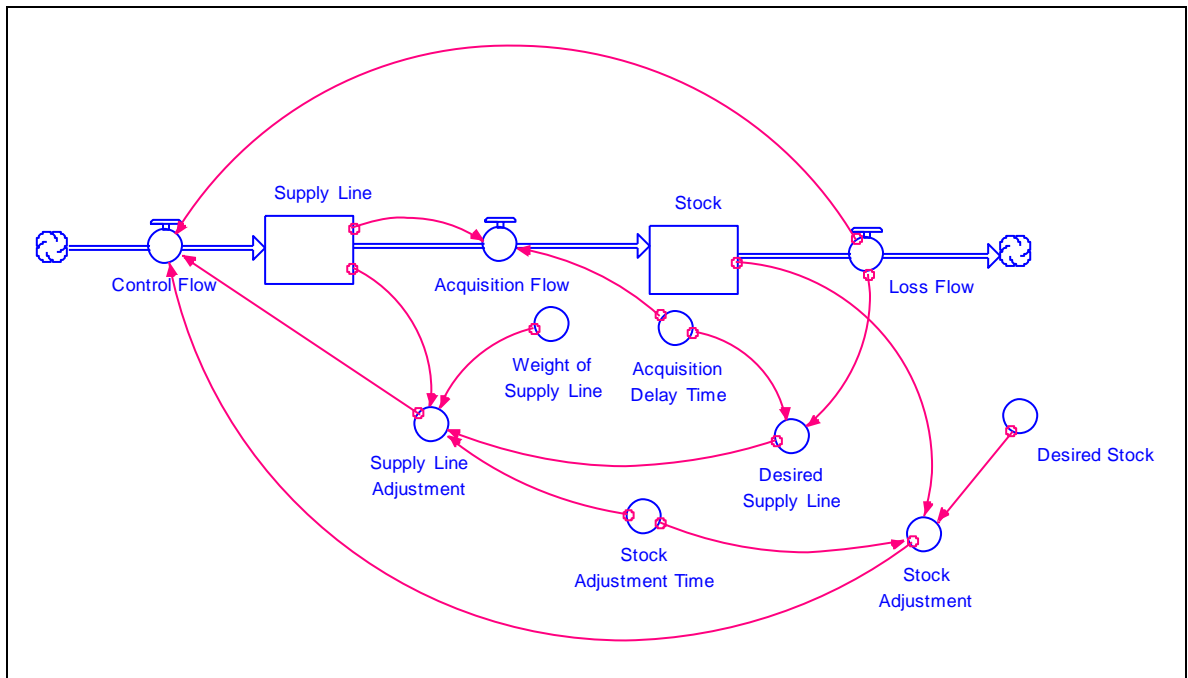


Figure 2.1. Stock management model with first order supply line.

The stock equations of this model are as follows:

$$SL_{t+DT} = SL_t + (CF_t - AF_t) \cdot DT \quad (2.1)$$

$$S_{t+DT} = S_t + \left(\frac{SL_t}{ADT} - LF_t \right) \cdot DT \quad (2.2)$$

The equations of the flows and the rest of the variables are given below:

$$CF = LF + SA + SLA \quad (2.3)$$

The control flow Equation 2.3 given above is called the anchor-and-adjust heuristic, which is widely used in stock management.

$$SA = \frac{S^* - S}{SAT} \quad (2.4)$$

$$SLA = w_{SL} \cdot \frac{SL^* - SL}{SAT} \quad (2.5)$$

$$AF = \frac{SL}{ADT} \quad (2.6)$$

$$LF = 0 \quad (2.7)$$

$$S^* = 0 \quad (2.8)$$

$$SL^* = LF \cdot ADT = 0 \quad (2.9)$$

Desired Stock and *Loss Flow* are taken to be zero, not only for the sake of simplicity but also for the similarity of the model to the soft landing model presented in this thesis. In an effort to obtain a second order differential equation for the stock-management model, we first obtained Equations 2.12 and 2.13 from Equations 2.1-2.2 and 2.10-2.11.

$$\dot{S} = \lim_{DT \rightarrow 0} \frac{S_{t+DT} - S_t}{DT} \quad (2.10)$$

$$\dot{SL} = \lim_{DT \rightarrow 0} \frac{SL_{t+DT} - SL_t}{DT} \quad (2.11)$$

$$\dot{S} = \frac{SL}{ADT} - LF \quad (2.12)$$

$$\dot{SL} = CF - AF \quad (2.13)$$

Later, we inserted Equations 2.3-2.9 into Equations 2.12-2.13 and simplified as shown below:

$$\dot{S} = \frac{SL}{ADT} \quad (2.14)$$

$$\dot{SL} = SA + SLA + LF - AF = \frac{-w_{SL} \cdot SL - S}{SAT} - \frac{SL}{ADT} \quad (2.15)$$

Finally, we transformed two first order differential equations (2.14-2.15) into a second order differential equation (Equation 2.19) as shown below.

$$\ddot{S} = \frac{\dot{S}L}{ADT} \quad (2.16)$$

$$\dot{S}L = \ddot{S} \cdot ADT \quad (2.17)$$

$$\ddot{S} \cdot ADT = \frac{-w_{SL} \cdot \dot{S} \cdot ADT - S}{SAT} - \dot{S} \quad (2.18)$$

$$ADT \cdot \ddot{S} + \left(1 + w_{SL} \cdot \frac{ADT}{SAT}\right) \cdot \dot{S} + \frac{1}{SAT} \cdot S = 0 \quad (2.19)$$

Equation 2.19 is used in Chapter 8 in developing the new heuristic proposed in this thesis.

3. THE SOFT LANDING MODEL

In this study, we first constructed a stock-flow model of the soft landing problem, which is given in Figure 3.1. This diagram represents only the physical structure of the soft landing problem; it does not represent the controller (e.g. a human decision maker, a computer). *Height* (i.e. the vertical distance between the spacecraft and landing surface) and *Velocity* (i.e. the vertical velocity) are the two stock variables (accumulations, system state variables) in the model, which are represented as boxes (see Figure 3.1). The stock Equations 3.2 and 3.4 are approximate integral equations. DT (simulation time step) in these equations is set to 2^{-9} (1/512) seconds, which is sufficiently small in emulating continuous time behavior. *Velocity*, which is a stock variable, is at the same time the one and only flow of *Height*. *Velocity* has a single flow too; *Acceleration*. In our model diagram (Figure 3.1) there are only two flows, which are represented by thick arrows with a valve in the middle. Flows, in general, define the rate that stocks change. Hence, *Height* is controlled via *Velocity*, *Velocity* via *Acceleration* (Equations 3.2 and 3.4). We select the initial conditions for the spacecraft so as to observe important dynamics that the model can generate (Equations 3.1 and 3.3). For example, if *Height* was set to a very low initial value, it would not be possible to observe how the vehicle behaves before it enters the very final stage of landing.

$$Height_0 = 1000 \quad [m] \quad (3.1)$$

$$Height_{t+DT} = Height_t + Velocity_t \cdot DT \quad [m] \quad (3.2)$$

$$Velocity_0 = -10 \quad [m/s] \quad (3.3)$$

$$Velocity_{t+DT} = Velocity_t + Acceleration \cdot DT \quad [m/s] \quad (3.4)$$

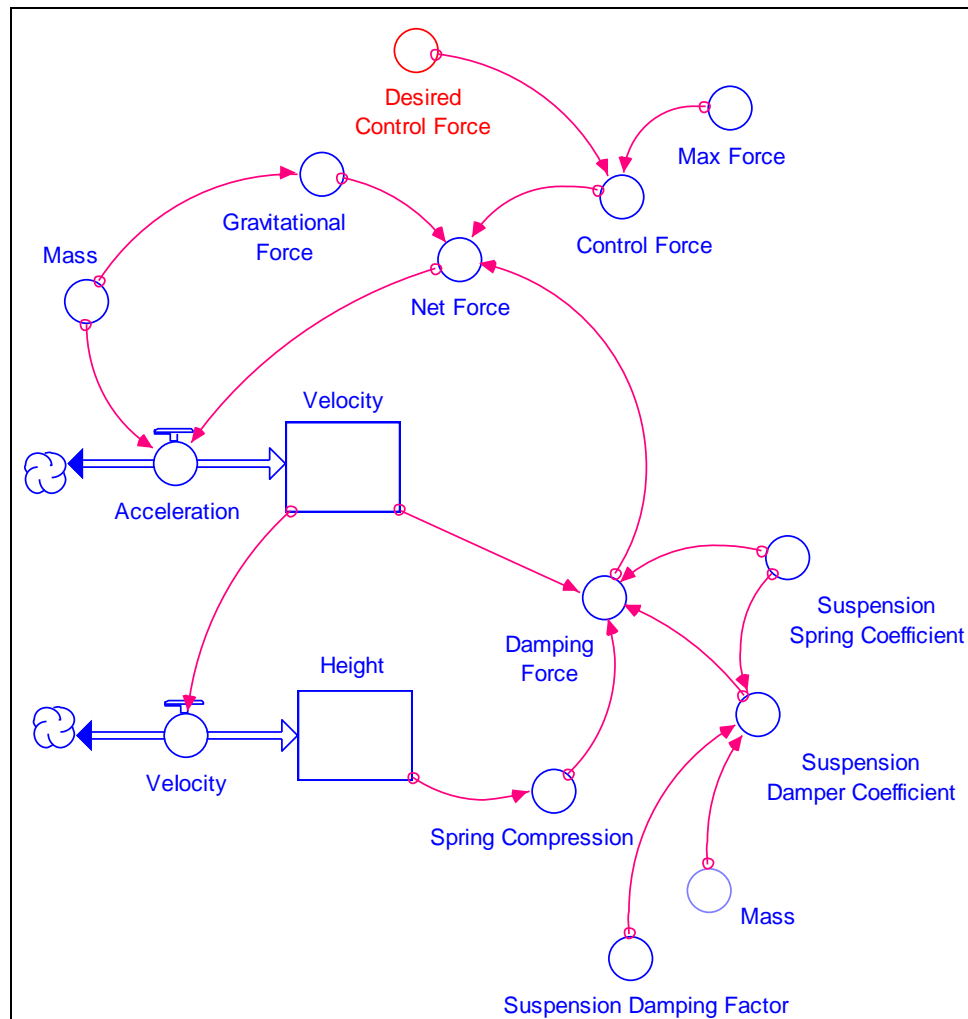


Figure 3.1. Stock-flow diagram of the model.

The thin arrows in Figure 3.1 represent causal functional relations that define the non-stock variables. Accordingly, *Net Force* and *Mass* determine *Acceleration* (Equation 3.5). In our model, *Mass* is a constant because we ignore the change in the mass due to fuel consumption (Equation 3.6). By doing so, we keep the model fairly simple to avoid an extra load of information that would complicate the essential understanding of the structure of the model. In Chapter 9, this assumption is relaxed in order to observe possible changes in the dynamics caused by a variable mass.

$$Acceleration = Net Force / Mass \quad [m/s^2] \quad (3.5)$$

$$Mass = 1000 [kg] \quad (3.6)$$

$$Net Force = Gravitational Force + Damping Force + Control Force \quad [N] \quad (3.7)$$

Height is controlled via *Velocity* (Equation 3.2), *Velocity* via *Acceleration* (Equation 3.4), *Acceleration* via *Net Force* (Equation 3.5), and *Net Force* via *Control Force* (Equation 3.7)². The control feedback loop structure also includes the controller, which determines *Control Force* via *Desired Control Force*. The natural inputs to the controller are *Height* and *Velocity*. A simplified causal loop diagram showing these relations and two negative (counteracting) feedback loops within the control feedback loop structure can be seen in Figure 3.2. Although, every control system involves delays in measuring/perceiving actual conditions (Yasarcan, 2011), we ignore such delays in our model for the sake of simplicity and assumed that the controller has instantaneous access to the current values of *Height* and *Velocity*. We also ignore delays caused by actuators. Explicitly modeling delays caused by actuators and measurement processes increases the model complexity (Atay, 2009; Barlas, 2002; Forrester, 1961; Forrester, 1971; Michiels and Niculescu, 2007; Sterman, 2000; Yasarcan, 2011; Yasarcan and Barlas, 2005).

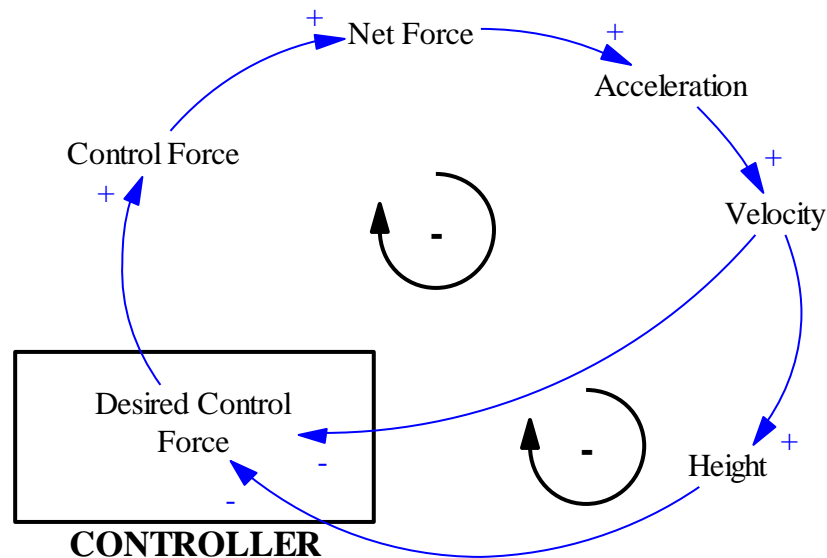


Figure 3.2. Causal-loop diagram of the control feedback loop structure.

Positive *Height*, *Velocity*, *Acceleration*, and force directions are upward from the surface. *Height* equals zero means that the vehicle touches the ground, but the springs of

² One Newton amounts to the force needed to increase the velocity of a one kilogram body of mass by one meter per second in one second ($N = \text{kg} \cdot \text{m} / \text{s}^2$).

the landing gear are at rest, so they bear no force at *Height* equals zero. Thus, when the vehicle comes to a static equilibrium, the springs of the landing gear get compressed balancing the weight (*Gravitational Force*) of the vehicle and *Height* becomes slightly less than zero. See the assumption regarding the *Suspension Spring Coefficient* at the end of this chapter.

Gravitational Force, *Damping Force*, and *Control Force* add up to the *Net Force* acting on the vehicle (Equation 3.7). *Gravitational Force* acts on the vehicle due to mass and gravity (Equation 3.8). *Gravitational Acceleration* is assumed to be constant during landing; in the model, it does not change with the distance to the surface (Equation 3.9). Corollary to constant *Mass* (Equation 3.6) and constant *Gravitational Acceleration* (Equation 3.9), *Gravitational Force* is also a constant (Equation 3.8).

$$\textit{Gravitational Force} = \textit{Mass} \cdot \textit{Gravitational Acceleration} [N] \quad (3.8)$$

$$\textit{Gravitational Acceleration} = -8.87 [m/s^2] \quad (3.9)$$

The gravitational acceleration of the celestial body to be landed on is assumed to be equal to the surface gravitational acceleration of Venus that is -8.87 m/s^2 (Equation 3.9). Note that the assumed landing conditions other than the gravitational acceleration do not resemble the conditions of Venus at all. Venus has a thick atmosphere, but we aimed to capture the difficulty caused by the absence of drag. Hence, we assumed zero drag force.

The landing gear of the spacecraft is comprised of dampers and springs. *Damping Force*, which is a result of the compression of the landing gear, is generated after the spacecraft contacts the landing surface (Equation 3.10). To be able to correctly represent the conditional existence of *Damping Force*, we also defined a variable named *Spring Compression*, which represents the amount of compression of the landing gear (Equation 3.11). Inclusion of *Spring Compression* is in accordance with our aim of obtaining a transparent model. *Suspension Spring Coefficient*, *Suspension Damper Coefficient*, and *Mass* determine the damping behavior, which can be subcritical, critical, or supercritical. The values of the two coefficients are selected such that a critically damped behavior is obtained after the touchdown (i.e. after the touchdown, *Height* asymptotically approaches to its equilibrium value).

$$Damping Force = \left\{ \begin{array}{l} 0, \\ \left(\begin{array}{l} Suspension \\ Spring \\ Coefficient \end{array} \right) \cdot \left(\begin{array}{l} Spring \\ Compression \end{array} \right) - \left(\begin{array}{l} Suspension \\ Damper \\ Coefficient \end{array} \right) \cdot Velocity, \text{ otherwise} \end{array} \right\} \left[N \right] \quad (3.10)$$

$$Spring Compression = \left(\begin{array}{l} 0, \\ -Height, \end{array} \begin{array}{l} Height \geq 0 \\ \text{otherwise} \end{array} \right) [m] \quad (3.11)$$

Desired Control Force determined by the controller, which is explained in Chapter 4, is an input to *Control Force* of the reverse force thruster. *Control Force* cannot be more than the maximum force applicable by the thruster (Equations 3.12 and 3.13).

$$Control Force = \left\{ \begin{array}{l} Desired Control Force, \\ Max Force, \end{array} \begin{array}{l} Desired Control Force \leq Max Force \\ \text{otherwise} \end{array} \right\} [N] \quad (3.12)$$

$$Max Force = 30,000 [N] \quad (3.13)$$

3.1. Selection of Landing Gear Parameters

Due to the final velocity at the instant of touchdown, the landing gear must bear some force. Depending on the amount of the final (landing) velocity, the selection of *Suspension Damping Ratio* (SDR) affects the force that the landing gear must bear. With higher SDR values, the amount of the force, when the landing velocity approaches to zero, decreases. However, with realistic landing velocities other than zero, a high SDR value causes a quick increase in the force that the landing gear must bear. It is possible to optimize SDR, given a landing velocity. For a comparison of optimum SDR values for given landing velocities see Table 3.1. We determined the desired final velocity as -2 m/s and selected -10 m/s as the boundary value between a hard landing and a crash. We used the optimum SDR value for -10 m/s to be able to account for a possible deviation from the desired velocity value. Choosing the optimum SDR value for -2 m/s would increase the

maximum force applied on the landing gear at a final velocity of -10 m/s by about 40% as compared to SDR's optimum value at this velocity, 0.3328. Thus, to be on the safe side, SDR is chosen as 0.3328 to minimize the force for the final velocity of -10 m/s. For comparison see Figure 3.3.

Table 3.1. Comparison of sample landing velocities and corresponding SDR values minimizing maximum force subjected to the landing gear.

Landing Velocity (m/s)	Optimum SDR value
-10	0.3328
-5	0.4070
-2	0.6644

$$\textit{Suspension Damping Ratio} = 0.3328 \quad [\text{unitless}] \quad (3.14)$$

$$\textit{Landing Gear Rest Compression} = 0.5 \quad [\text{m}] \quad (3.15)$$

$$\textit{Suspension Spring Coefficient} = 17,740 \quad [\text{N} / \text{m}] \quad (3.16)$$

$$\textit{Suspension Damper Coefficient} t = 2,803 \quad \left[\frac{\text{N} \cdot \text{s}}{\text{m}} \right] \quad (3.17)$$

Landing Gear Rest Compression is the amount of the compression in the springs caused solely by the weight of the spacecraft on the target celestial body. Together with *Gravitational Force* and *Mass*, it determines the value of *Suspension Spring Coefficient* and *Suspension Damper Coefficient*.

$$\textit{Suspension Spring Coefficient} = - \frac{\textit{Gravitational Force}}{\textit{Landing Gear Rest Compression}} \quad [\text{N} / \text{m}] \quad (3.18)$$

$$\textit{Suspension Damper Coefficient} t = 2 \cdot \left\{ \textit{Suspension Damping Ratio} \cdot \sqrt{\left(\frac{\textit{Suspension Spring Coefficient}}{\textit{Coefficient} t} \right) \cdot \textit{Mass}} \right\} \quad \left[\frac{\text{N} \cdot \text{s}}{\text{m}} \right] \quad (3.19)$$

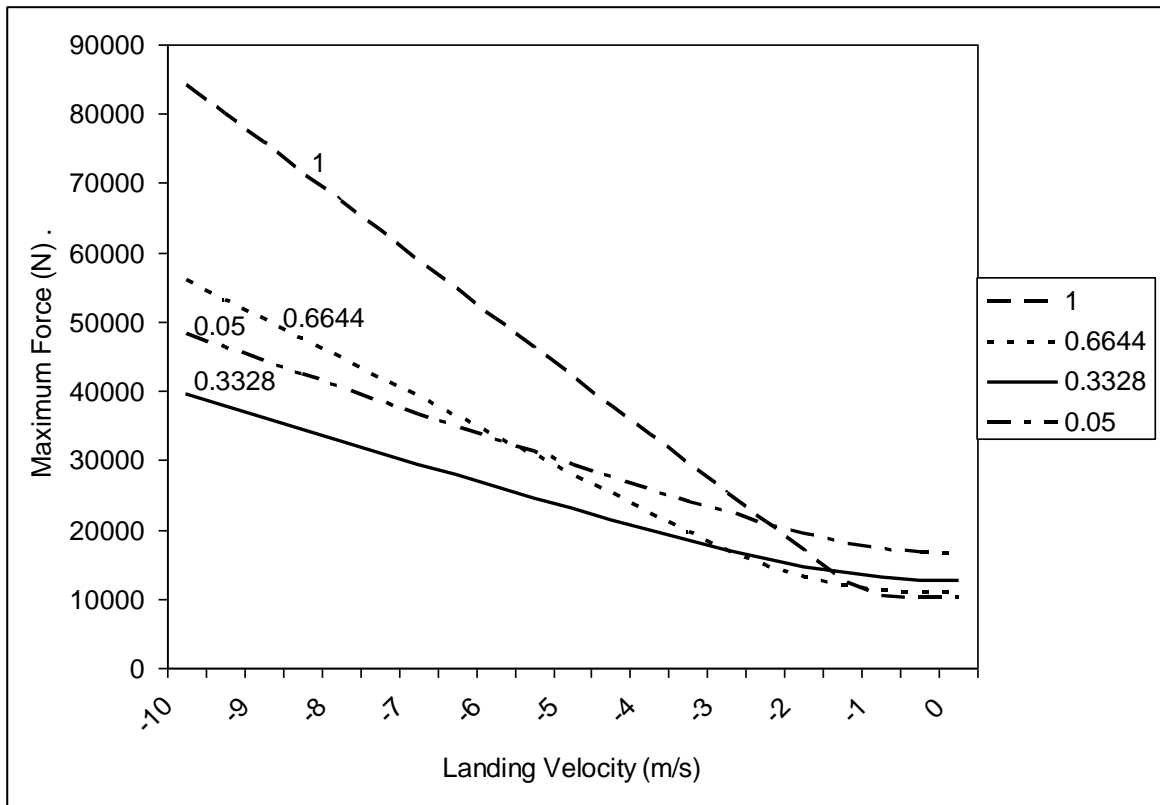


Figure 3.3. *Maximum Landing Force* variation with different *Landing Velocity* values displayed on five *Suspension Damping Ratio* Values.

3.2. Simplifying Model Assumptions

The summary of the simplifying model assumptions are given below:

- The movement of the spacecraft in the horizontal axes is not modeled. Spacecraft is assumed to move only vertically.
- There is no atmosphere in the landing area, thus no air friction exists that would cause a drag force on the vehicle (Equation 3.7).
- *Gravitational Acceleration* is assumed to be constant during landing; it does not change with the distance to the surface (Equation 3.9).
- *Mass* is a constant, the change in the mass due to fuel consumption is ignored (Equation 3.6).
- The landing gear has fixed specifications; *Suspension Spring Coefficient* and *Suspension Damper Coefficient* are both constants.
- *Suspension Spring Coefficient* is selected so that the equilibrium value for *Spring*

Compression is 0.5 meters (i.e. the equilibrium value for *Height* is -0.5 meters).

- *Suspension Damper Coefficient* is selected so as to minimize *Maximum Landing Force* for *Landing Velocity* of -10 m/s. The selected value is less than one, which creates underdamped behavior (i.e. after the touchdown, the vehicle shows slight damping oscillations around its equilibrium height value).
- There are no delays caused by actuators; *Desired Control Force* generated by the controller affects *Control Force* without a time lag (Equation 3.12).
- Information flow from the system to the controller is perfect and instantaneous; there are no errors or delays caused by measurement processes.

3.3. Performance Measures

Performance measure equations are used to evaluate the landing. *Landing Time* gives the duration of the landing beginning with the initial conditions until the moment of touchdown (Equations 3.20-3.21). *Landing Velocity* is the velocity value at the moment of touchdown (Equations 3.22-3.23). *Max Landing Force* reports the maximum force that is generated by the landing gear after touchdown (Equations 3.24-3.25). *Force Ratio* gives a scale of *Maximum Landing Force* comparing it to *Gravitational Force* (Equation 3.26). Note that at static equilibrium the landing gear withstands *Gravitational Force*. *Max Acceleration* gives the maximum acceleration of the vehicle during landing (Equations 3.27-3.28). *Number of Sign Change in Force* counts the directional change of force and consequently also acceleration (Equations 3.29-3.30).

$$LandingTime_0 = 0 \quad [s] \quad (3.20)$$

$$LandingTime_{t+DT} = LandingTime_t + \begin{cases} t, & LandingTime_t = 0, Height_t < 0 \\ 0, & otherwise \end{cases} \quad [s] \quad (3.21)$$

$$LandingVelocity_0 = 0 \quad [m/s] \quad (3.22)$$

$$\begin{aligned} \left(\begin{array}{c} Landing \\ Velocity \end{array} \right)_{t+DT} &= \\ \left(\begin{array}{c} Landing \\ Velocity \end{array} \right)_t &+ \begin{cases} Velocity_t, & LandingVelocity_t = 0, Height_t < 0 \\ 0, & otherwise \end{cases} \quad [m/s] \end{aligned} \quad (3.23)$$

$$MaxLandingForce_0 = 0 \quad [N] \quad (3.24)$$

*Max Landing Force*_{t+DT} =

$$\left(\begin{array}{c} \text{Max} \\ \text{Landing} \\ \text{Force} \end{array} \right)_t + \left\{ \begin{array}{l} \left(\begin{array}{c} \text{Damping Force}_t \\ -\text{Max Landing Force}_t \end{array} \right), \left(\begin{array}{c} \text{Damping} \\ \text{Force} \end{array} \right)_t > \left(\begin{array}{c} \text{Max Landing} \\ \text{Force} \end{array} \right)_t \\ 0, \quad \text{otherwise} \end{array} \right\} [N] \quad (3.25)$$

$$\text{Force Ratio} = \frac{\text{Maximum Landing Force}}{-\text{Gravitational Force}} \quad [\text{unitless}] \quad (3.26)$$

$$\text{Max Accelerati on}_0 = 0 \quad [m/s^2] \quad (3.27)$$

*Max Accelerati on*_{t+DT} =

$$\text{Max Accelerati on}_t \quad (3.28)$$

$$+ \left\{ \begin{array}{l} \left(\begin{array}{c} \text{Accelerati on}_t \\ -\text{Max Accelerati on}_t \end{array} \right), \text{Accelerati on}_t > \left(\begin{array}{c} \text{Max} \\ \text{Accelerati on} \end{array} \right)_t \\ 0, \quad \text{otherwise} \end{array} \right\} [m/s^2]$$

$$\text{Number of Sign Change in Force until Landing}_0 = 0 \quad [\text{unitless}] \quad (3.29)$$

*Number of Sign Change in Force until Landing*_{t+DT} =

$$\left\{ \begin{array}{l} \left(\begin{array}{c} \text{Number of Sign} \\ \text{Change in Force} \\ \text{until Landing} \end{array} \right)_t + 1, \quad \text{Net Force}_t \cdot \text{Net Force}_{t+DT} < 0 \\ \left(\begin{array}{c} \text{Number of Sign} \\ \text{Change in Force} \\ \text{until Landing} \end{array} \right)_t, \quad \text{otherwise} \end{array} \right\} [\text{unitless}] \quad (3.30)$$

$$\left(\begin{array}{c} \text{Instantaneous} \\ \text{Change in Net Force} \end{array} \right)_{t+DT} = \text{ABS}(\text{Net Force}_{t+DT} - \text{Net Force}_t) [N] \quad (3.31)$$

*Max Instantaneous Change in Net Force*_{t+DT} =

$$\text{Max Instantaneous Change in Net Force}_t + \quad (3.32)$$

$$\left\{ \begin{array}{l} \left(\begin{array}{c} \text{Instant} \\ \text{aneous} \\ \text{Change in} \\ \text{Net Force} \end{array} \right)_t - \left(\begin{array}{c} \text{Max} \\ \text{Instantaneous} \\ \text{Change in} \\ \text{Net Force} \end{array} \right)_t, \left(\begin{array}{c} \text{Instant} \\ \text{aneous} \\ \text{Change in} \\ \text{Net Force} \end{array} \right)_t > \left(\begin{array}{c} \text{Max} \\ \text{Instantaneous} \\ \text{Change in} \\ \text{Net Force} \end{array} \right)_t \\ 0, \quad \text{otherwise} \end{array} \right\} [N]$$

$$\text{Max Instantaneous Change in Net Force}_0 = 0 \quad [N] \quad (3.33)$$

4. A MASS-SPRING-DAMPER BASED CONTROL HEURISTIC

The stock-flow model given in Figure 3.1 represents only the physical structure of the soft landing problem. In this chapter, a mass-spring-damper based (MSD) heuristic is assumed to be used by the controller in producing the values for *Desired Control Force*. In essence, this heuristic is a PD (proportional-derivative) controller. The simulated behavior generated by the model and the heuristic is discussed in the next chapter. The aim of this chapter is to present the formulations of this heuristic.

Yasarcan and Barlas (2005) use a procedure in developing control heuristics for control problems involving information delay or indirect control via a secondary-stock. This procedure adapts a well known successful heuristic for control problems involving material supply line delay, using the similarity of the differential equations of control problems involving different types of delay structures. The model presented in Chapter 3 can be reduced to a second order linear differential equation because it contains two stock variables, which are defined by approximate integral equations (Equation 3.2 and Equation 3.4). The mass-spring-damper model is well studied and it is known how to obtain a certain behavior by adjusting the model parameter values. Furthermore, it can also be represented by a second order linear differential equation. The heuristic is developed based on the similarity of the differential equations of the mass-spring-damper model and the model presented in the previous chapter³.

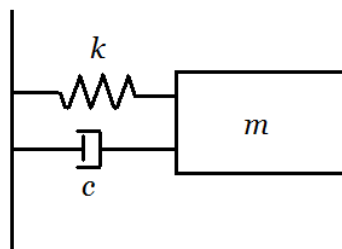


Figure 4.1. Mass-spring-damper schematic.

³ The authors of this paper acknowledge that it is Dr. I. Emre Köse who suggested to us to use the mass spring damper model for this purpose.

The schematic given in Figure 4.1 is a well known one. The differential equation of a non-driven (i.e. $F_{external} = 0$) mass-spring-damper model with mass m , spring constant k , and damper coefficient c is given below:

$$m \cdot \ddot{x} + c \cdot \dot{x} + k \cdot x = 0 \quad (4.1)$$

In Equation 4.1, x represents displacement, \dot{x} represents velocity, and \ddot{x} represents acceleration. This equation can be described by using stock-flow concepts, x and \dot{x} being the stocks and their associated flows being \dot{x} and \ddot{x} respectively. Note that \dot{x} is a flow and a stock at the same time. As a further clarification, $-k \cdot x$ is the spring force (F_{spring}) and $-c \cdot \dot{x}$ is the damper force (F_{damper}). The net force applied on the body of mass is the sum of these two forces ($F_{net} = F_{damper} + F_{spring} = -c \cdot \dot{x} - k \cdot x$). According to Newton's second law of motion mass times acceleration is equal the net force acting on the body ($F_{net} = m \cdot \ddot{x}$). Therefore, mass times acceleration is equal to the sum of the spring force and damper force. Hence, Equation 4.1 is obtained.

The damping ratio of the mass-spring-damper model is:

$$Damping\ Ratio = \frac{c}{2 \cdot \sqrt{m \cdot k}} \quad (4.2)$$

The dynamics of the mass-spring-damper model can be underdamped, overdamped, or critically damped depending on the value of *Damping Ratio*. For *Damping Ratio* values under 1, the dynamic behavior is underdamped and for values over 1, it is overdamped. The case where *Damping Ratio* is exactly 1 is called critically damped. When the dynamic behavior is underdamped, the spring dominates the movement and the body of mass oscillates. In the critically damped case, the body asymptotically approaches the rest condition without an overshoot. In the overdamped case, the damper dominates the dynamics and the body approaches the rest condition slower compared to the critically damped case (Åström and Murray, 2008). As a summary, the importance of *Damping Ratio* is that determining its value determines the dynamics of the mass-spring-damper model.

The suggested control heuristic is adapted from the mass-spring-damper model that is defined by Equation 4.1. *Height*, *Velocity*, *Acceleration*, and *Mass* in our model corresponds to x , \dot{x} , \ddot{x} , and m in Equation 4.1, respectively. In the heuristic, we named k as *Height Coefficient* and c as *Velocity Coefficient*. Thus, Equation 4.1 becomes:

$$Mass \cdot Acceleration + \left(\frac{Velocity}{Coefficient} \right) \cdot Velocity + \left(\frac{Height}{Coefficient} \right) \cdot Height = 0 \quad (4.3)$$

Utilizing Newton's second law of motion, the following can be written:

$$Desired\ Net\ Force = - \left(\frac{Velocity}{Coefficient} \right) \cdot Velocity - \left(\frac{Height}{Coefficient} \right) \cdot Height \quad [N] \quad (4.4)$$

The reverse force thruster should also counteract *Gravitational Force*. Hence, *Desired Control Force*, which is the output of the heuristic and an input to *Control Force* (see Equation 3.12 and Figure 3.1), can be given as:

$$Desired\ Control\ Force = Desired\ Net\ Force - Gravitational\ Force \quad [N] \quad (4.5)$$

$$Height\ Coefficient = 10 \quad [N/m] \quad (4.6)$$

$$Velocity\ Coefficient = 200 \quad [N \cdot s/m] \quad (4.7)$$

The parameters of the adapted heuristic, *Height Coefficient* and *Velocity Coefficient* values are set to 10 $[N/m]$ and 200 $[N \cdot s/m]$, respectively. Consequently, the damping ratio for our model becomes:

$$Damping\ Ratio = \frac{Velocity\ Coefficient}{2 \cdot \sqrt{Mass \cdot Height\ Coefficient}} = \frac{200}{2 \cdot \sqrt{1000 \cdot 10}} = 1 \quad (4.8)$$

The value of *Damping Ratio* means that the suggested control heuristic produces a critically damped behavior for the height of the spacecraft. If *Damping Ratio* was less than 1, this would imply a possible overshoot ($Height < 0$). This is equivalent to saying that the

vehicle can continue its normal motion below the ground level, which is not possible. Therefore, in the soft landing model, if *Damping Ratio* is less than 1, a crash may occur. On the other hand, a slower approach would also be undesired. Therefore, the heuristic parameters are selected so that *Damping Ratio* becomes 1. For the simulated dynamics of the soft landing model with the proposed heuristic, see Section 4.3.

4.1. Selection of the Controller Parameters

Decreasing *Damping Ratio* shortens the landing duration and increases the final velocity (See Figure 4.2). Long landing durations and also great final velocity values should be avoided. Therefore, a *Damping Ratio* value with a reasonable landing duration and final (landing) velocity should be selected. The final velocity should be less than -10 m/s to be able to obtain a safe landing, so *Damping Ratio* should minimally be 0.8. *Damping Ratio* value 1 has a special mathematical significance; it is the minimal value that makes the vehicle asymptotically⁴ seek the ground level and is not affected by the initial conditions. Due to this mathematical property, *Damping Ratio* is taken as 1.

⁴ To be mathematically correct, asymptotical seek of the goal takes indefinite time. This issue will be addressed in the next sub-section.

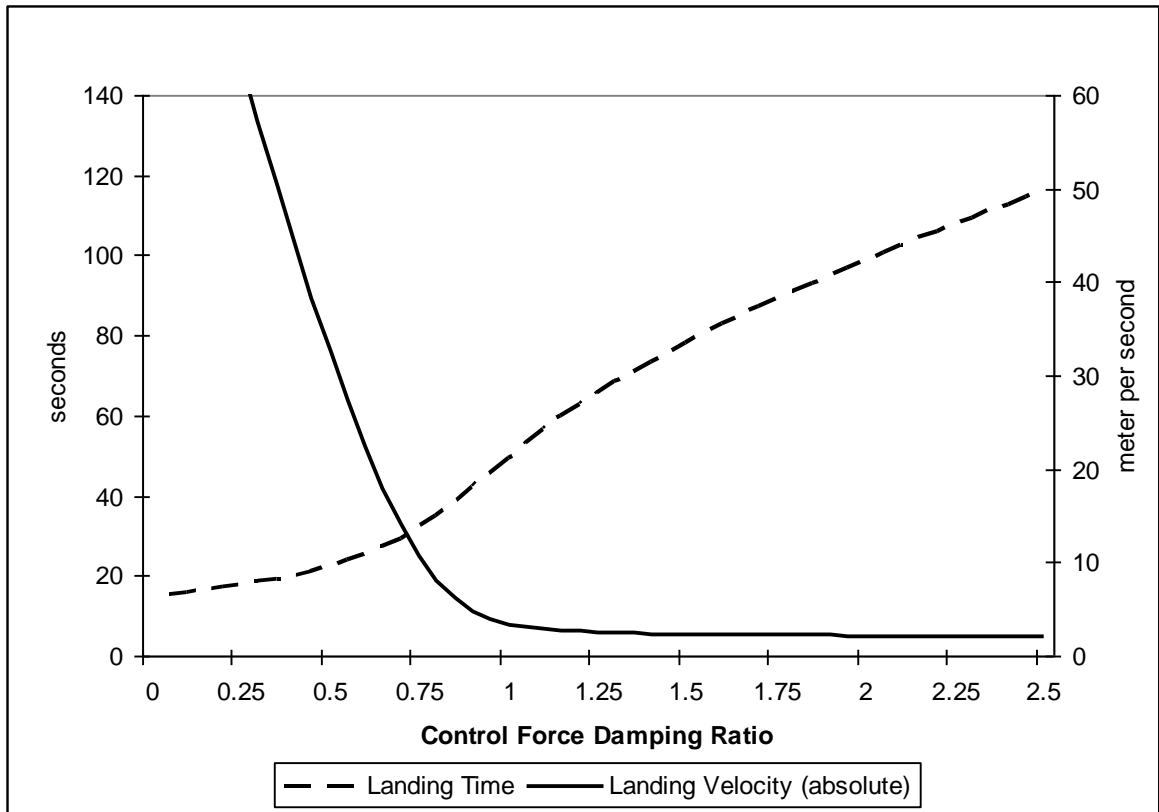


Figure 4.2. Landing Time and Absolute Landing Velocity variation with different Control Force Damping Ratios.

4.2. Adjustments to the Mass-Spring-Damper Based Heuristic

As mentioned in the previous section, there is a problem with the asymptotical approach of the heuristic with *Damping Ratio* = 1. The vehicle continues to hover on the ground, a very small distance away from the surface. Additionally, the heuristic should stop controlling after the first touchdown.

We used an adjusted version of Equation 4.5 so that upon touching the ground, the thruster is off and is not switched on again. Equation 4.4 implicitly assumes that the heuristic seeks *Velocity* = 0. We also changed this assumption by defining a constant named *Desired Final Velocity*. These assumptions lead to the following equations:

Desired Net Force =

$$-\left(\begin{array}{c} \text{Velocity} \\ \text{Coefficient } t \end{array}\right) \cdot \left(\begin{array}{c} \text{Velocity} - \left(\begin{array}{c} \text{Desired} \\ \text{Final} \\ \text{Velocity} \end{array}\right) \end{array}\right) - \left(\begin{array}{c} \text{Height} \\ \text{Coefficient } t \end{array}\right) \cdot \text{Height} \quad [N] \quad (4.9)$$

$$\text{Desired Final Velocity} = -1.2 \quad [m/s] \quad (4.10)$$

The existence of a negative *Desired Final Velocity* means that the vehicle asymptotically seeks the ground level with a velocity, so the problem of the infinite duration due to the asymptotical seek is avoided.

Landing State is an important structure within the model, which is included in some performance measures' evaluation (Equations 4.11-4.12). It also serves the purpose of preventing the heuristics from trying to control the vehicle after the landing has occurred (Equation 4.13).

$$\text{Landing State}_0 = 0 \quad [\text{unitless}] \quad (4.11)$$

*Landing State*_{*t+DT*} =

$$\text{Landing State}_t + \left(\begin{array}{c} 1, \\ 0, \end{array} \begin{array}{l} \text{Landing State}_t = 0, \text{ Height}_t < 0 \\ \text{otherwise} \end{array}\right) \quad [\text{unitless}] \quad (4.12)$$

$$\left(\begin{array}{c} \text{Desired} \\ \text{Control} \\ \text{Force} \end{array}\right) = \left\{ \begin{array}{l} \left(\begin{array}{c} \text{Desired} \\ \text{Net Force} \end{array}\right) - \left(\begin{array}{c} \text{Gravitational} \\ \text{Force} \end{array}\right), \\ 0, \end{array} \begin{array}{l} \text{Landing State} = 0 \\ \text{Landing State} = 1 \end{array} \right\} \quad [N] \quad (4.13)$$

4.3. Dynamic Behavior of Landing

As described previously, *Height* is controlled via *Velocity* (Equation 3.2), *Velocity* via *Acceleration* (Equation 3.4), *Acceleration* via *Net Force* (Equation 3.5), and *Net Force* via *Control Force* (Equation 3.7). The control feedback loop structure also includes the controller, which determines *Control Force* applied by the reverse force thruster via *Desired Control Force* (Figure 3.2). In order to obtain a reasonable value for *Desired Control Force*, the controller should consider the system state variables (i.e. *Height* and *Velocity*). Only by doing so is it possible to reach the aim of landing the spacecraft as

gently and as fast as possible. Recall that we intentionally left out many real life complexities in order to keep the model simple. Even under simplifying assumptions, the control task still is not a straightforward one. Despite the fact that one of our simplifying assumptions is that the values of the state variables *Height* and *Velocity* are measured/perceived instantaneously and without error, it is necessary to develop a proper control heuristic⁵. The main reason for the difficulty is that the control task requires simultaneous control of *Height* and *Velocity*, which -due to the physical structure of the problem- can only be indirectly affected by the reverse force thruster; *Height* and *Velocity* have inertia; their values do not change instantaneously (see Figures 1.1 and 3.1 and Equations 3.1-3.7). The addition of delays caused by actuators to the model would further complicate the control task by amplifying the effect of the modeled inertia⁶.

The stock-flow model given in Figure 3.1 and defined by Equations 3.1-3.13 describes the structure of the soft landing problem excluding the controller. The formulations of the heuristic suggested for the controller is explained in Chapter 4. The dynamic behavior presented in Figures 4.3-4.7 is generated by simulating the model including the controller with the proposed heuristic for 60 seconds (Equations 3.1-3.13 and Equations 4.4-4.5).

The dynamic behavior of *Height* is given in Figure 4.3. Initially, the change in *Height* (i.e. *Velocity*) is relatively fast and, as the spacecraft approaches to the surface, the change in *Height* slows down. This behavior is comparable to the landing behavior of Apollo 15 (see Figure 1.2). Hence, one can conclude that the behavior obtained by the control heuristic is a reasonable one; by a fast initial decline, the heuristic tries to decrease the time to land; by a slow final approach, it keeps the impact force well below harmful values. At the instant of touchdown, the value of *Velocity* is -2.04 meters per second (-7.35 km/h) creating a maximum impact force of circa 14,782 Newton, approximately 1.67 times the weight of the spacecraft on the target celestial body (8,870 Newton). The weight corresponds to the model variable *Gravitational Force*, which is the force that the landing

⁵ For example, see Yasarcan (2011) for the significance of and difficulties introduced by measurement or perception delays.

⁶ For example, see Yasarcan and Barlas (2005) for different types of delays between *Desired Control Force* and *Control Force* (i.e. delay between “control flow” and “acquisition flow”, and delay between “desired control flow” and “control flow”), and the effects of these delays.

gear must bear when the spacecraft is standing still on the ground. The discussion on the strength design of the spacecraft is beyond the scope of this study.

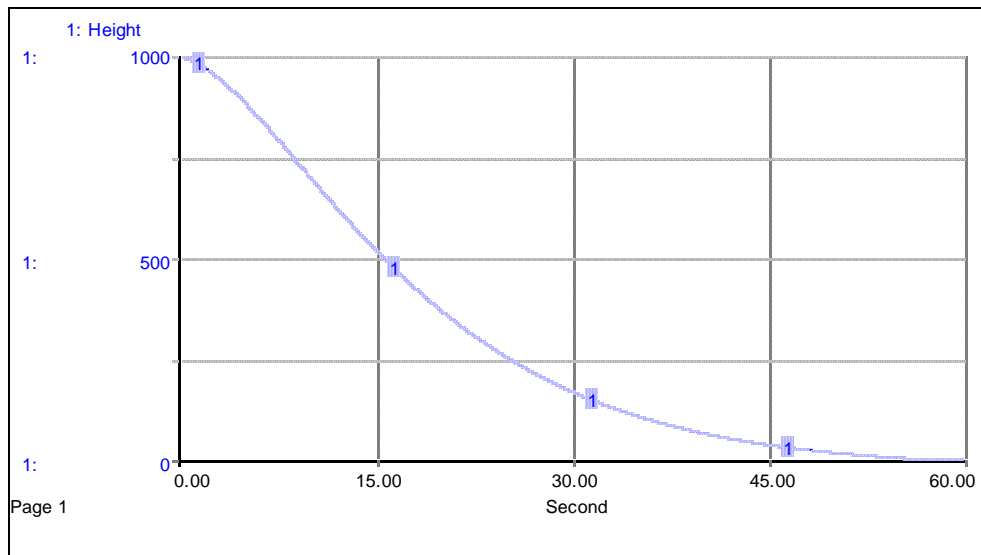


Figure 4.3. Dynamic behavior of *Height*.

The dynamic behavior of *Velocity* and *Net Force* acting on the vehicle during landing are given in Figures 4.4 and 4.5, which further explain the dynamic behavior obtained by the control heuristic. At first, the heuristic allows the spacecraft to accelerate in the negative direction towards the landing surface (see Figure 4.4, approximately within the time range of 0-10 seconds) by keeping *Net Force* negative (i.e. *Control Force* less than *Gravitational Force*, see Figures 4.5 and 4.6). Aiming to decrease the duration of landing, *Velocity* continues to increase during this initial period. After this initial phase, *Velocity* decreases until the vehicle touches the surface (see Figure 4.4, approximately within the time range of 10-55 seconds). In this later phase, the heuristic produces more *Control Force* than *Gravitational Force* (Figure 4.5) resulting in a positive *Net Force* (Figure 4.6). At the moment of landing, *Control Force* is turned off and *Damping Force*, which is zero throughout the simulation up to this point, takes over and stops the vehicle (see Figures 4.5 and 4.6, approximately around 55 seconds).

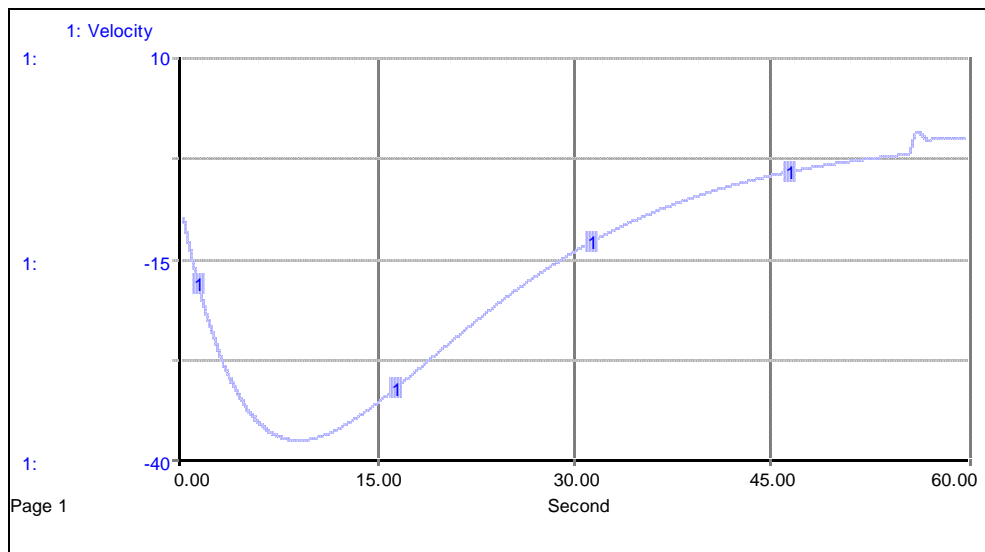
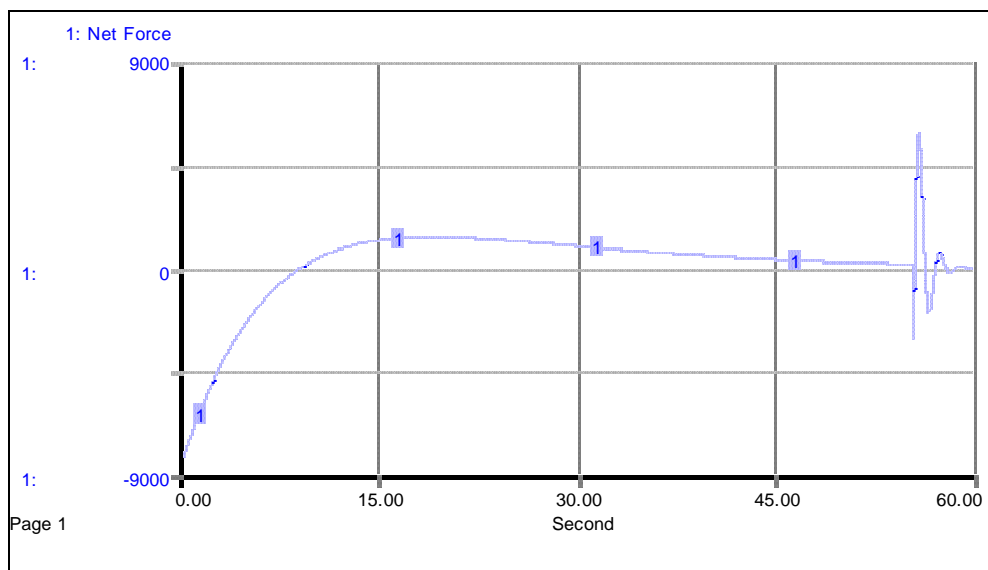
Figure 4.4. Dynamic behavior of *Velocity*.

Figure 4.5. Net force acting on the vehicle during landing.

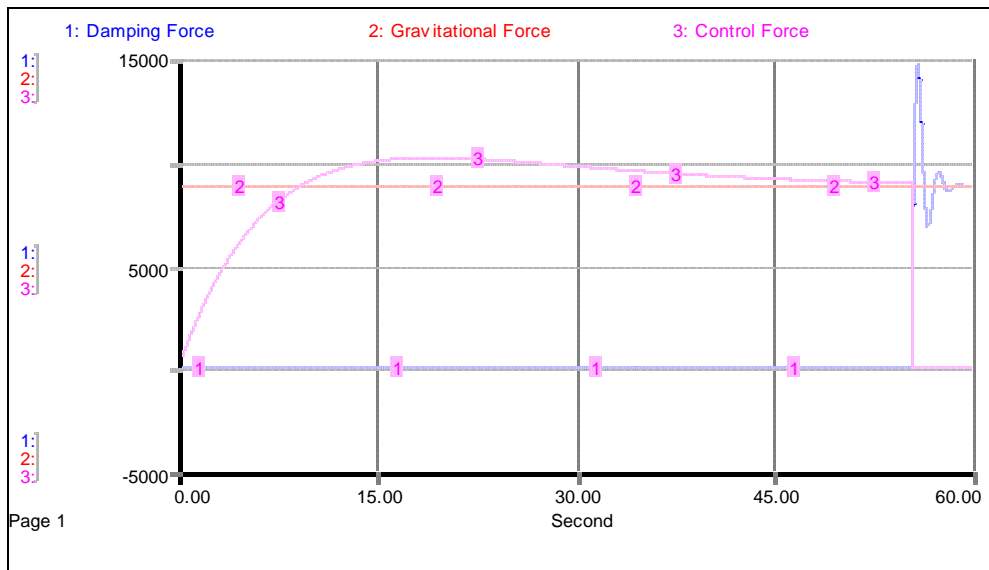


Figure 4.6. Absolute values of the forces acting on the vehicle during landing.

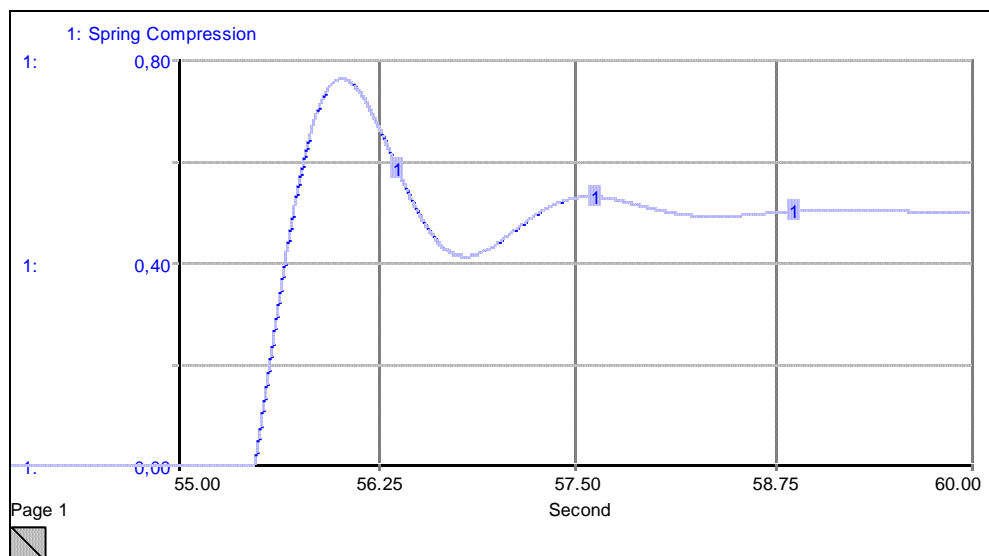


Figure 4.7. Dynamic behavior of *Spring Compression* during the final process of landing (between seconds 55-60).

5. BANG-BANG CONTROL HEURISTIC

The bang-bang principle relies on the fact that a system can be controlled in minimal time properly using all available power throughout the whole control. A bang-bang system is defined as a system that utilizes maximum power for control at all times. Additionally, for systems with one degree of freedom there is an optimal one. This optimal one, if it exists, is also the best of all possible systems in terms of minimal time (LaSalle, 1959).

A bang-bang control type heuristic was developed for our model. The purpose is to let the vehicle descend up to a certain *Height* with only the effect of *Gravitational Force* in an accelerating fashion, and then apply the maximum possible force until touchdown. Note that; in our model, *Control Force* is in the positive *Height* direction and *Gravitational Force* is the only force in the negative direction that can pull the vehicle to the ground.

$$\begin{aligned}
 & \text{Desired Control Force} = \\
 & \left\{ \begin{array}{ll} \text{Max Force,} & \text{Velocity}^2 - \left(\begin{array}{l} \text{Desired} \\ \text{Final} \\ \text{Velocity} \end{array} \right)^2 > 2 \cdot \text{Height} \cdot \left(\begin{array}{l} \text{Maximum} \\ \text{Possible} \\ \text{Acceleration} \end{array} \right) \\ \\ 0, & \text{otherwise} \end{array} \right\} [N] \quad (5.1)
 \end{aligned}$$

$$\text{Desired Final Velocity} = -2 \quad [m/s] \quad (5.2)$$

$$\left(\begin{array}{l} \text{Maximum Possible} \\ \text{Acceleration} \end{array} \right) = (\text{Max Force} + \text{Gravitational Force}) / \text{Mass} \quad [m/s^2] \quad (5.3)$$

It is possible to determine the critical point after which the application of the maximum force can decelerate the vehicle to the desired approach velocity. Up to this critical point the vehicle accelerates as much as possible with the *Gravitational Force* acting on the vehicle. Based on the work-energy principle, equating kinetic energy at the critical point to the kinetic energy at the final moment and the work done on the vehicle after the critical point, this point can be determined (see Equations 5.4 and 5.5).

$$\frac{1}{2} m \cdot v_c^2 = \frac{1}{2} m \cdot v_f^2 + m \cdot a_{\max} \cdot x_c \quad [J] \quad (5.4)$$

$$v_c^2 - v_f^2 = 2 \cdot a_{\max} \cdot x_c \quad [m^2 / s^2] \quad (5.5)$$

When the critical distance is reached, *Desired Net Force* becomes *Max Force*; decelerating the vehicle until touchdown (see also Equations 4.4, 3.12-3.13, 5.1-5.3). Furthermore; with the determined initial condition, it is also possible to calculate the point, as of which *Max Force* application is necessary (See Appendix A). Note that, the modified *Desired Control Force* equation 4.13 and *Landing State* Equations 4.11-4.12 are also valid in the bang-bang heuristic.

The dynamic behavior of *Height* is given in Figure 5.1. Initially, the change in *Height* (i.e. *Velocity*) is relatively fast and, as the spacecraft approaches to the surface, the change in *Height* slows down. At the instant of touchdown, the value of *Velocity* is -3.28 meters per second (-11.81 km/h) creating a maximum impact force of circa 17,869 Newton, approximately 2.01 times the weight of the spacecraft on the target celestial body (8,870 Newton). Note that, *Landing Velocity* value -3.28 m/s obtained by the bang-bang heuristic is due to a numerical error by the Euler Method used in the simulation. Ideally, when time step is infinitesimally small, *Landing Velocity* would approach *Desired Final Velocity* value of -2 m/s.

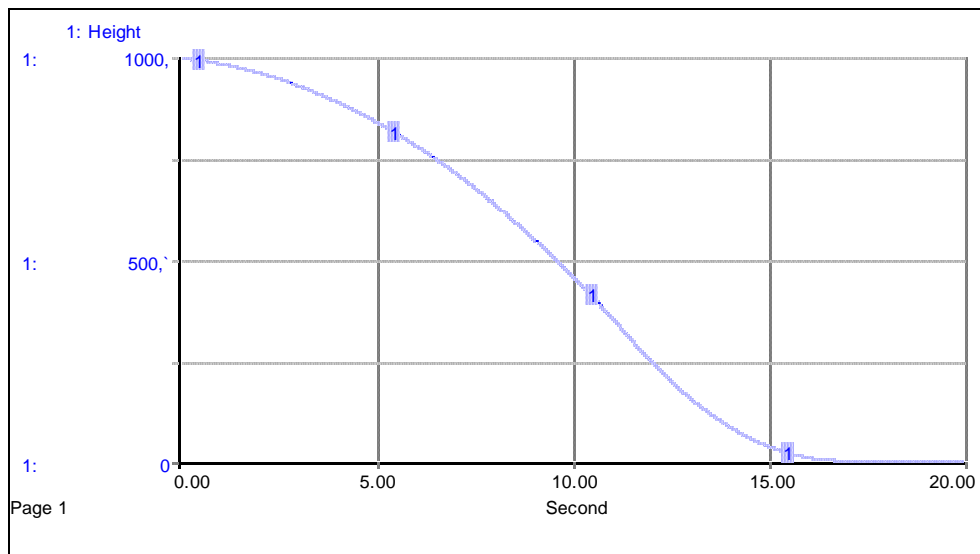


Figure 5.1. Dynamic behavior of *Height* in the bang-bang heuristic.

The dynamic behavior of *Velocity* and *Net Force* acting on the vehicle during landing are given in Figures 5.2 and 5.3, which further explain the dynamic behavior obtained by the control heuristic. At first, the heuristic allows the spacecraft to accelerate with the effect of *Gravitational Acceleration* in the negative direction towards the landing surface (see Figure 5.2, approximately within the time range of 0-12 seconds) by keeping *Net Force* equal to *Gravitational Force* (see Figures 5.3 and 5.4). Aiming to decrease the duration of landing, *Velocity* continues to increase during this initial period. After this initial phase, *Velocity* decreases until the vehicle touches the surface (see Figure 5.2, approximately within the time range of 12-17 seconds). In this later phase, the heuristic produces *Control Force* equal to *Max Force* (Figure 5.3) resulting in a positive *Net Force* (Figure 5.4). At the moment of landing, *Control Force* is turned off and *Damping Force*, which is zero throughout the simulation up to this point, takes over and stops the vehicle (see Figures 5.3 and 5.4, approximately around 17 seconds).

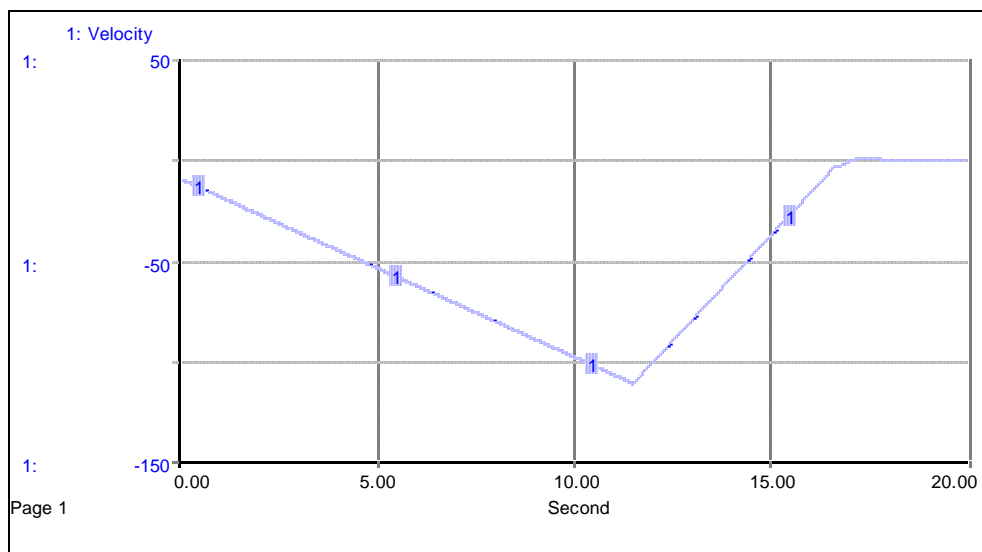


Figure 5.2. Dynamic behavior of *Velocity*.

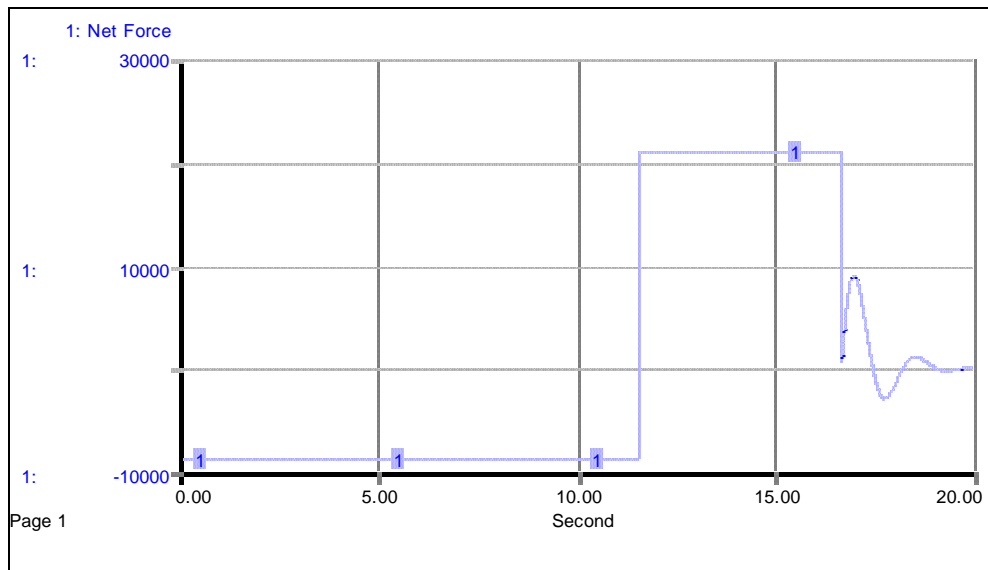


Figure 5.3. Net force acting on the vehicle during landing.

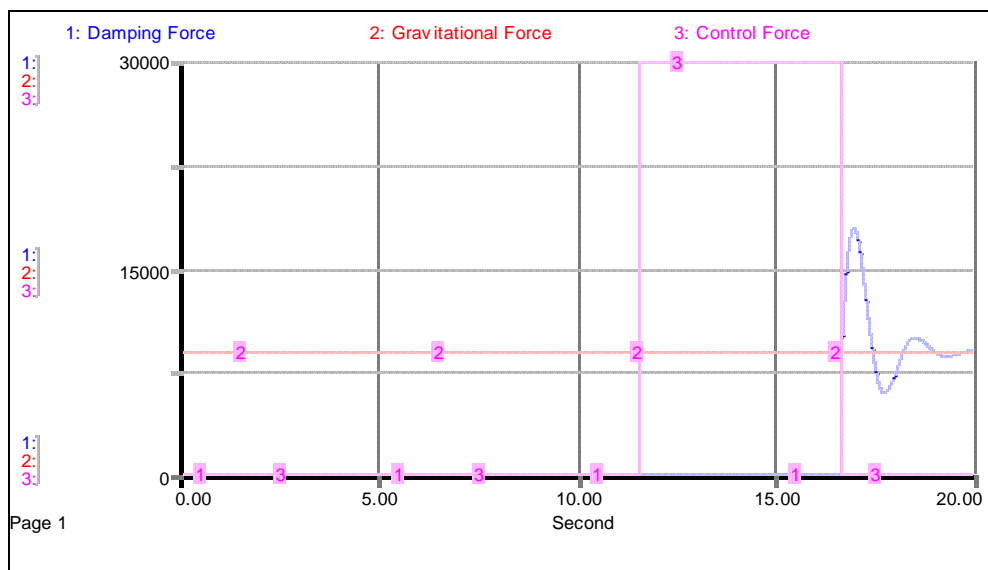


Figure 5.4. Absolute values of the forces acting on the vehicle during landing.

6. A NEW HEURISTIC

In this chapter, we have developed a new heuristic, combining the previously discussed mass-spring-damper (MSD) and bang-bang heuristics and, additionally, it includes the concept “weight of supply line” borrowed from stock management discussed in Chapter 2.

The two-stock soft landing model (Figure 3.1) incorporating the mass-spring-damper heuristic (given in Chapter 4), excluding nonlinearities caused by *Max Force* limitation and touchdown processes, is similar to a second order stock management model (given in Chapter 2); they can both be reduced to a second order linear differential equation. Remembering Equation 2.19 from the generic stock management structure when anchor-and-adjust heuristic is used in control and Equation 4.3 of the soft landing model when mass-spring-damper heuristic is used in control:

$$ADT \cdot \ddot{S} + \left(1 + w_{SL} \cdot \frac{ADT}{SAT}\right) \cdot \dot{S} + \frac{1}{SAT} \cdot S = 0$$

$$Mass \cdot Acceleration + \left(\frac{Velocity}{Coefficient}\right) \cdot Velocity + \left(\frac{Height}{Coefficient}\right) \cdot Height = 0$$

We can match the variables of Equations 2.19 and 4.3:

$$Mass = ADT \tag{6.1}$$

$$Height\ Coefficient = \frac{1}{SAT} \tag{6.2}$$

$$Velocity\ Coefficient = 1 + w_{SL} \cdot \frac{ADT}{SAT} \tag{6.3}$$

Implementing the coefficients of the generic stock management structure, the equation for the new heuristic becomes:

$$ADT \cdot Acceleration + \left(1 + w_{SL} \cdot \frac{ADT}{SAT}\right) \cdot Velocity + \frac{1}{SAT} \cdot Height = 0 \quad (6.4)$$

The difference between mass-spring-damper heuristic and the anchor-and-adjust heuristic lies in the calculation of *Velocity Coefficient*. Mass-spring-damper heuristic determines the coefficients by setting *Damping Ratio* to 1, so that critically damped behavior is obtained. In stock management, however, *Weight of Supply Line* of the anchor-and-adjust heuristic is usually set to 1 in order to guarantee non-oscillatory behavior (Serman, 1989; Yasarcan, 2011; Yasarcan and Barlas, 2005). Note that, this rule ensures that the obtained behavior is not underdamped as shown by equation 6.6.

Damping Ratio, which is given by Equation 4.2, can also be expressed as given below using the equivalency Equations 6.1-6.3:

$$Damping Ratio = \frac{1}{2} \cdot \left(\sqrt{\frac{SAT}{ADT}} + w_{SL} \cdot \sqrt{\frac{ADT}{SAT}} \right) \quad (6.5)$$

If *Weight of Supply Line* = 1, Equation 6.5 becomes:

$$Damping Ratio = \frac{1}{2} \cdot \left(\sqrt{\frac{SAT}{ADT}} + \sqrt{\frac{ADT}{SAT}} \right) \geq 1 \quad (6.6)$$

In the new heuristic, we use the following equation for *Velocity Coefficient*, which is obtained by using the equivalency Equations 6.1 and 6.2 and setting *Weight of Supply Line* = 1 in Equation 6.3:

$$Velocity Coefficient = 1 + Mass \cdot Height Coefficient \quad (6.7)$$

Remember that, in mass-spring-damper heuristic, the selection of *Height Coefficient* as 10 and *Damping Ratio* as 1 (critical damping) equates *Velocity Coefficient* to 200 as previously given in Chapter 4. In the new heuristic, the selection of *Height Coefficient* as 10 and *Weight of Supply Line* as 1, gives *Velocity Coefficient* of 10,001. The mass-spring-

damper based heuristic would necessitate extensive amount of landing time for this new value of *Velocity Coefficient*. In order to prevent this unwanted behavior, instead of using *Desired Final Velocity* (Equation 4.10) in the equation of *Desired Net Force* (Equation 4.9), we define a new variable called *Desired Velocity* which is a dynamically calculated variable (i.e. the value of *Desired Velocity* is calculated for each *Height* value). We derive the formulation for *Desired Velocity* (Equation 6.8) from Equation 5.5, on which the bang-bang heuristic (Equation 5.1) relies, as well. Thus, in this way, we combine the two heuristics.

$$Desired\ Velocity = -\sqrt{2 \cdot \frac{\left(\begin{array}{c} Behavior \\ Smoothing \\ Factor \end{array} \right) \cdot \left(\begin{array}{c} Positive \\ Available \\ Net\ Force \end{array} \right) \cdot Height}{Mass}} + \left(\begin{array}{c} Desired \\ Final \\ Velocity \end{array} \right) [m/s] \quad (6.8)$$

Similar to the adjusted *Desired Net Force* equation of the mass-spring-damper heuristic (Equation 4.9), the *Desired Net Force* equation for the new heuristic becomes:

$$Desired\ Net\ Force = -\left(\begin{array}{c} Velocity \\ Coefficient \end{array} \right) \cdot \left(Velocity - \left(\begin{array}{c} Desired \\ Velocity \end{array} \right) \right) - \left(\begin{array}{c} Height \\ Coefficient \end{array} \right) \cdot Height \quad [N] \quad (6.9)$$

$$Desired\ Control\ Force = Desired\ Net\ Force - Gravitational\ Force \quad [N] \quad (6.10)$$

Behavior Smoothing Factor determines the fraction of the *Positive Available Net Force* to be used in the calculation of *Desired Velocity* (Equation 6.8). Note that, *Behavior Smoothing Factor* = 0 would not allow proper control and would set the *Desired Velocity* equal to *Desired Final Velocity* at all *Height* values, whereas *Behavior Smoothing Factor* = 1 would make the new heuristic approach the bang-bang heuristic.

$$Positive\ Available\ Net\ Force = Max\ Force + Gravitational\ Force \quad [N] \quad (6.11)$$

$$Behavior\ Smoothing\ Factor = 0.25 \quad [unitless] \quad (6.12)$$

$$Desired\ Final\ Velocity = -0.5 \quad [m/s] \quad (6.13)$$

This heuristic achieves landing in 22.55 seconds with *Landing Velocity* -1.99 m/s. The dynamic behavior of the landing achieved by the new heuristic is given in figures below.

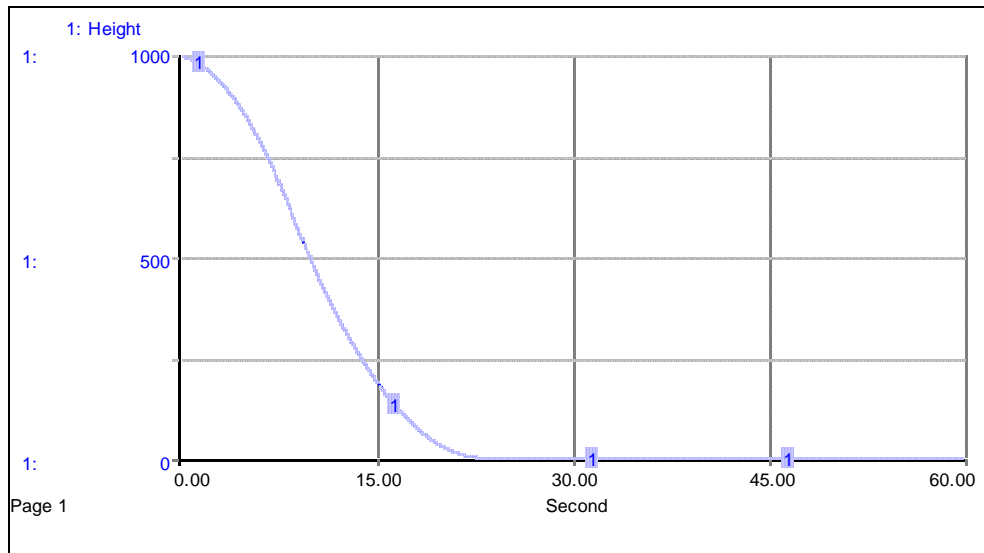


Figure 6.1. Dynamic behavior of *Height*.

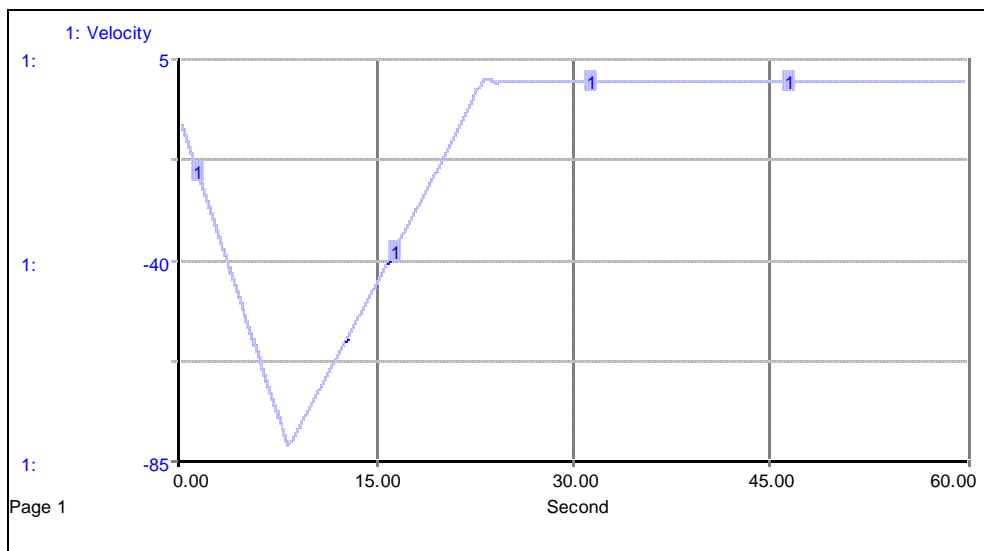


Figure 6.2. Dynamic behavior of *Velocity*.

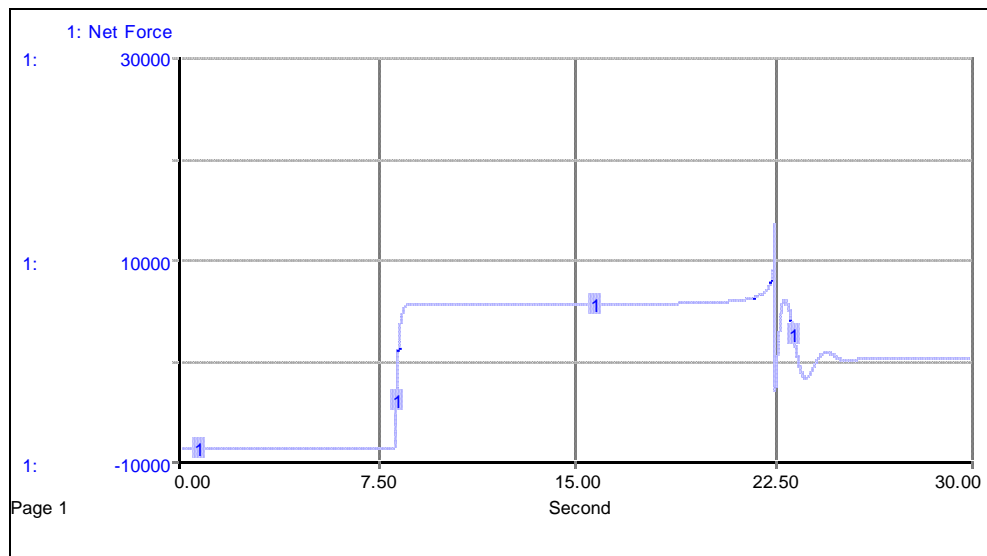


Figure 6.3. Net force acting on the vehicle during landing.

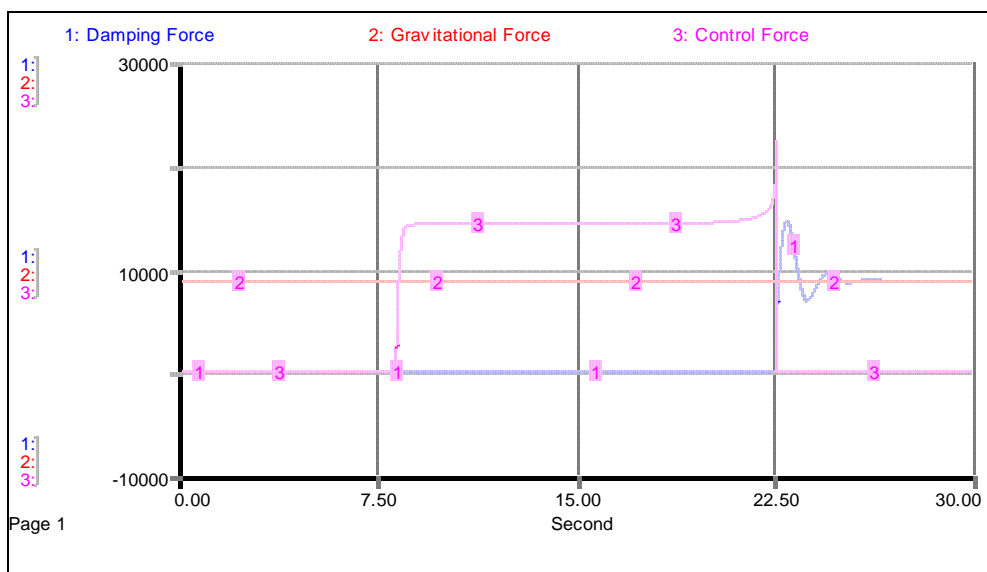


Figure 6.4. Absolute values of the forces acting on the vehicle during landing.

7. TERMINAL GUIDANCE HEURISTIC FOR VERTICAL MOVEMENT

In this chapter, a non-linear heuristic was adapted for the control of the vehicle during descent. The non-linear heuristic was simplified from Kriegsman and Reiss (1962).

The remaining time required to reach the surface at any point during landing can be roughly approximated as *Height/Velocity*. Although this approximation disregards the value of *Acceleration*, approaching the surface the term *Height/Velocity* converges to the real value of the remaining time.

Using the difference between *Velocity* and *Desired Final Velocity* and the remaining time, formulated as *Height/Velocity*, *Command Acceleration* can be calculated as:

$$\text{Command Acceleration} = \left(\text{Velocity} - \left(\frac{\text{Desired Final Velocity}}{\text{Height}} \right) \right) \cdot \frac{\text{Velocity}}{\text{Height}} \quad [m/s^2] \quad (7.1)$$

From the above equation, we can write the following for the *Desired Control Force*:

$$\left(\frac{\text{Desired Control Force}}{\text{Mass}} \right) = \frac{(\text{Velocity} - \text{Desired Final Velocity}) \cdot \text{Velocity}}{\text{Height}} \quad [N] \quad (7.2)$$

$$\text{Desired Final Velocity} = -1.8 \quad [m/s] \quad (7.3)$$

In the simulation runs, an adjusted version of Equation 7.2 is used. This form of the equation may result in the occurrence of a division-by-zero error in the final moments of the approach. For this purpose, the value of *Height/Velocity* is set to -0.01 for *Height* values smaller than 0.01. The modified equation becomes:

Desired Control Force =

$$\left\{ \begin{array}{l} \frac{(Velocity - Desired\ Final\ Velocity) \cdot Velocity \cdot Mass}{Height}, \quad Height \geq 0.01 \\ \frac{(Velocity - Desired\ Final\ Velocity) \cdot Mass}{-0.01}, \quad Height < 0.01 \end{array} \right\} [N] \quad (7.4)$$

The dynamic behavior of *Height* is given in Figure 7.1. Initially, the change in *Height* (i.e. *Velocity*) is relatively fast and, as the spacecraft approaches to the surface, the change in *Height* slows down. At the instant of touchdown, the value of *Velocity* is -2.05 meters per second (-7.38 km/h) creating a maximum impact force of circa 14,796 Newton, approximately 1.67 times the weight of the spacecraft on the target celestial body (8,870 Newton).

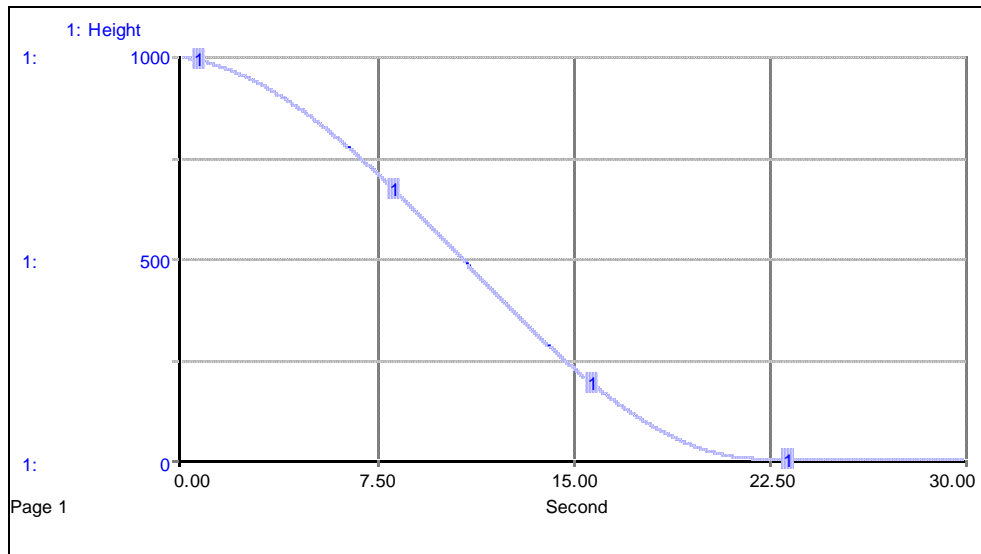


Figure 7.1. Dynamic behavior of *Height* in the terminal guidance heuristic.

The dynamic behavior of *Velocity* and *Net Force* acting on the vehicle during landing are given in Figures 7.2 and 7.3, which further explain the dynamic behavior obtained by the control heuristic. At first, the heuristic allows the spacecraft to accelerate towards the landing surface (see Figure 7.2, approximately within the time range of 0-10 seconds) with the effect of *Gravitational Acceleration* by keeping *Desired Control Force* less than *Gravitational Force* (see Figures 7.3 and 7.4). Aiming to decrease the duration of landing, *Velocity* continues to increase during this initial period. After this initial phase, *Velocity*

decreases until the vehicle touches the surface (see Figure 7.2, approximately within the time range of 10-22 seconds). In this later phase, the heuristic produces *Control Force* greater than *Gravitational Force* (Figure 7.3) resulting in a positive *Net Force* (Figure 7.4). At the moment of landing, *Control Force* is turned off and *Damping Force*, which is zero throughout the simulation up to this point, takes over and stops the vehicle (see Figures 7.3 and 7.4, approximately around 22 seconds).

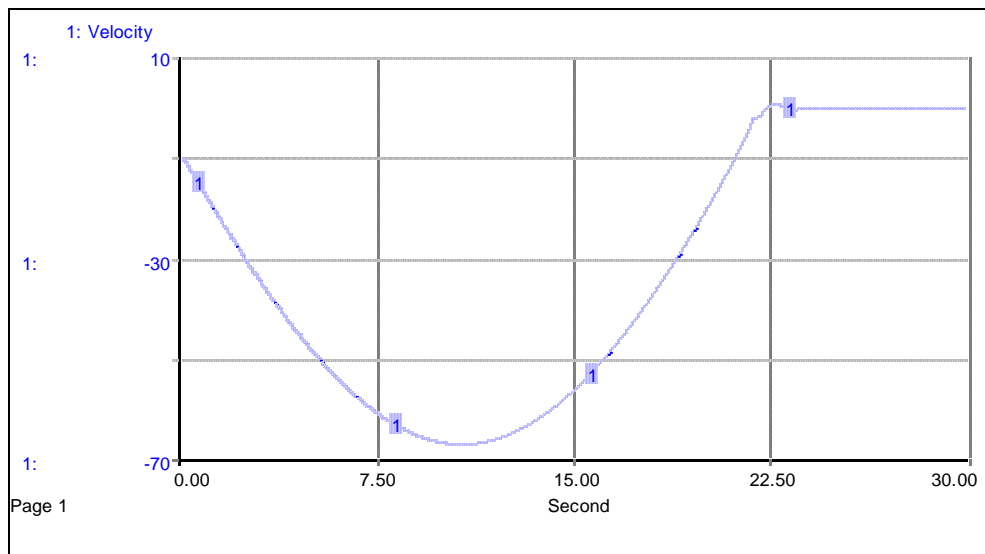


Figure 7.2. Dynamic behavior of *Velocity*.

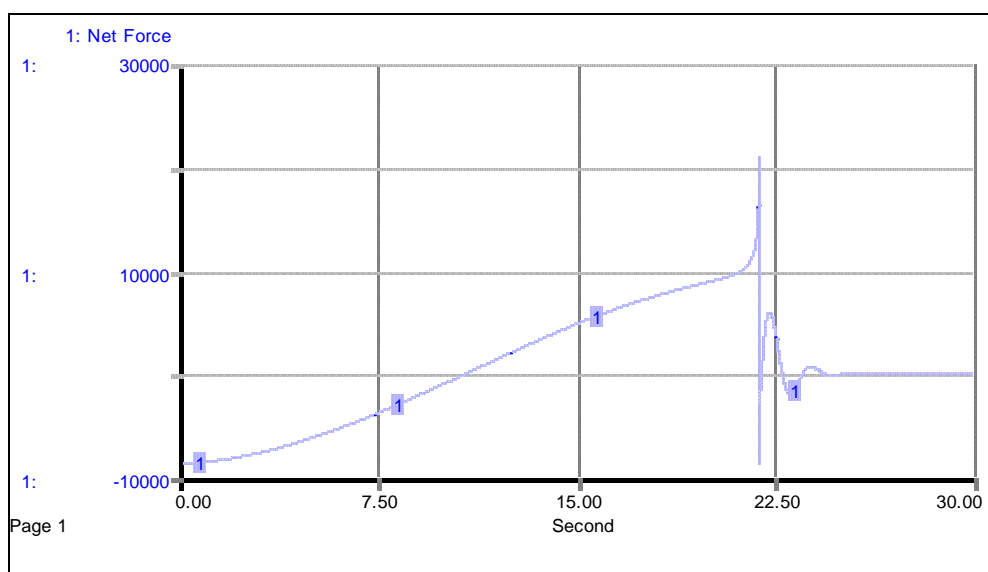


Figure 7.3. Net force acting on the vehicle during landing.

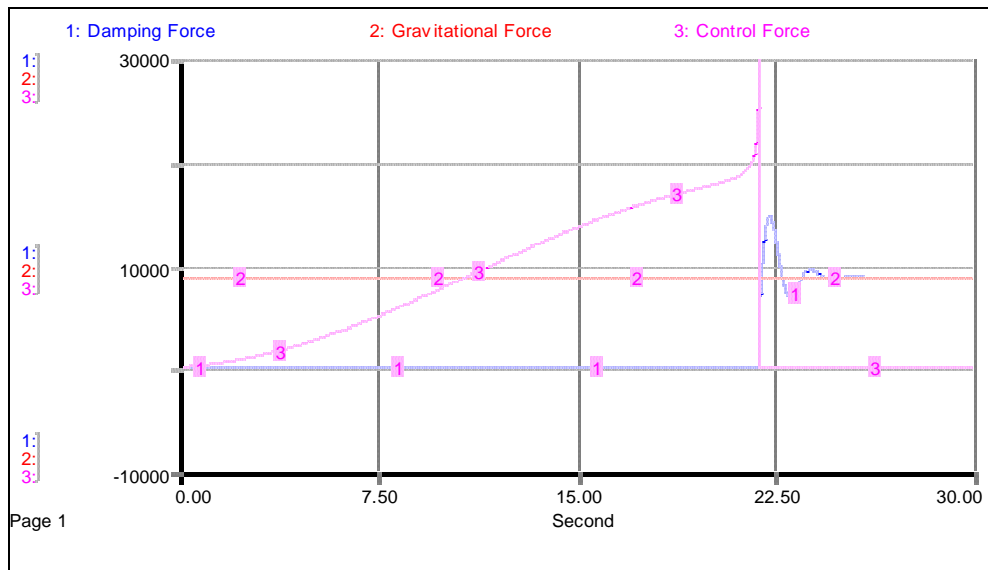


Figure 7.4. Absolute values of the forces acting on the vehicle during landing.

8. COMPARISON OF THE HEURISTICS AND THE SENSITIVITY OF THE HEURISTICS TO DEVIATIONS FROM THE MODEL ASSUMPTIONS

The mass-spring-damper (MSD) heuristic, the bang-bang heuristic, the new heuristic, and the terminal guidance heuristic presented in the previous chapters have different characteristics. The differences between the four heuristics and the differences in the resulting behaviors are explained in this chapter. A summary of the comparison of the heuristics is given in Table 8.1.

Table 8.1. Comparison of the four heuristics.

	MSD	bang-bang	new heuristic	terminal guidance
<i>Landing Time</i>	55.46	16.66	22.55	21.86
<i>Landing Velocity</i>	-2.04	-3.28 ⁷	-1.99	-2.05
<i>Max Landing Force</i>	14782	17869	14677	14796
Changes in <i>Control Force</i>	smooth	catastrophic	smooth	smooth
Operating Range	limited	limited only in the presence of errors and delays	limited only in the presence of errors and delays	limited only in the presence of errors and delays
Sensitivity to errors in parameters	low	high	low	low
Sensitivity to variable readings	low	high	medium	medium
Sensitivity to a relatively minor actuator delay time	low	very high	high	medium-high

The qualitative comparison of the velocity Figures 4.4, 5.2, 6.2, and 7.2 gives a preliminary insight to the difference in the smoothness of the control. Furthermore, the comparison of the net force Figures 4.5, 5.3, 6.3, and 7.3 reveals that the bang-bang control heuristic makes a sudden jump in the force, the new heuristic and the terminal guidance heuristic show a quick increase in force, whereas the mass-spring damper heuristic changes force gradually. The performance measure equations for *Max Instantaneous Change in*

⁷ The difference between the *Desired Final Velocity* and *Landing Velocity* obtained by the bang-bang heuristic is due to numerical errors caused by simulation. *Landing Velocity* would approach *Desired Final Velocity* if the simulation time step would be shorter.

Force (Equations 3.32 and 3.33) quantify momentary difference in force as 30,000 Newton in the bang-bang heuristic, 563.9 Newton in the terminal guidance heuristic, 278 Newton in the new heuristic and 3.4 Newton in the mass-spring-damper heuristic. In the mass-spring-damper heuristic, the new heuristic and the terminal guidance heuristic, however, *Max Instantaneous Change in Force* is only existent due to the discrete nature of the simulation; it approaches zero as DT goes to zero.

An additional difference, which is not directly observable from the graphical comparison, is that the bang-bang heuristic and the new heuristic have information about the vehicle, its *Max Force* per se. The bang-bang heuristic basically determines the point of force application and applies maximum force from that point on until the landing occurs. Where the mass-spring-damper heuristic and the terminal guidance heuristic may generate *Desired Control Force* values that are greater than *Max Force*; the bang-bang heuristic and the new heuristic would not do so, as they rely on *Max Force* to create the *Control Force*. Additionally, a general comparison of the heuristics' force utilization during landing can be seen from Figure 8.1. The constant maximum force use of the bang-bang heuristic is easily observed from this graph. Another important observation is the flatness of the force profile of mass-spring-damper heuristic and that *Net Force* decreases towards the end of landing, whereas *Net Force* increases in both the new heuristic and the terminal guidance heuristic in the final moments before the landing.

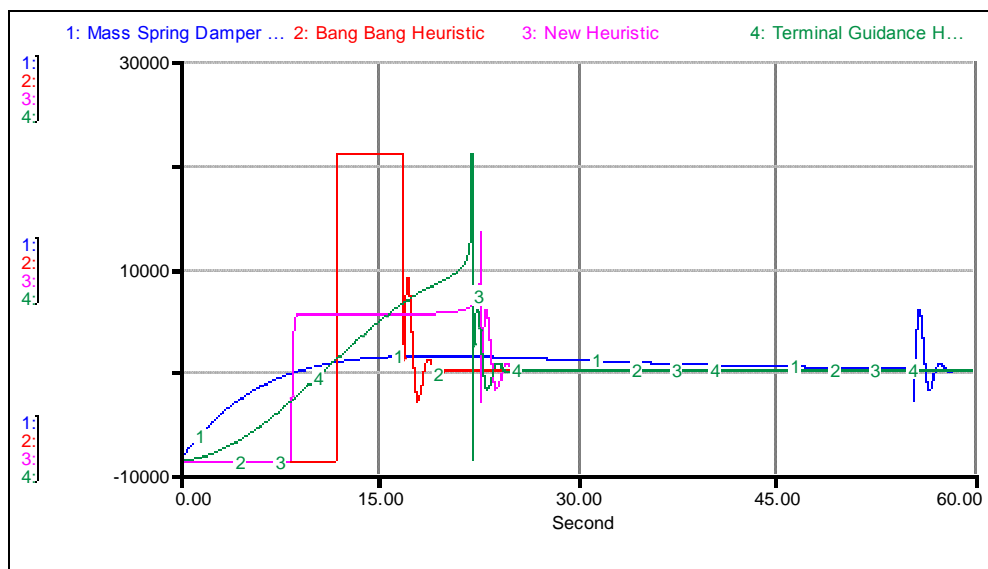


Figure 8.1. Net Force profiles generated by the heuristics.

Landing Velocity is another important criterion like *Landing Time*, and Equations 3.22 and 3.23 are necessary for monitoring it. In our simulations with a time step of 2^{-9} (1/512) seconds, the bang-bang heuristic, the mass-spring-damper heuristic, the new heuristic, and the terminal guidance heuristic landed with velocities of -3.28 m/s, -2.04 m/s, -1.99 m/s, and -2.05 m/s; respectively. At this point, it is worth noting that the *Landing Velocity* of the bang-bang heuristic would decrease, if a shorter simulation time step is used. Therefore, the difference between the *Landing Velocity* of the bang-bang heuristic and the *Landing Velocity* values of the other heuristics is not an actual difference, it is a simulation error.

A major drawback of the mass-spring-damper heuristic is that the landing behavior is affected by the selection of the initial conditions. Depending on the initial conditions and the value of *Height Coefficient*, the mass-spring-damper heuristic may require *Control Force* values far greater than *Max Force*. This may cause for the heuristic to let the vehicle accelerate towards the surface for too long, possibly causing a crash. This indicates a limited operating range with the set parameters of the heuristic.

Looking at Table 8.1, another difference is the time the heuristics need to complete the landing. The performance measure equations for *Landing Time* (Equations 3.20 and 3.21) aid this comparison. The bang-bang heuristic takes about 17 seconds to complete the landing with the given initial conditions; the terminal guidance heuristic completes the landing in about 22 seconds, the new heuristic takes about 23 seconds, and the mass-spring-damper heuristic needs about 55 seconds. In fact, it is expected that the bang-bang heuristic is the minimum-time solution for a problem of this sort. Note that, decreasing the time to land and equivalently minimizing the fuel consumption are one of the main goals of the heuristics. Naturally, as the bang-bang heuristic is time-optimal, it performs better regarding these criteria. However, it should also be noted that, this optimality exists only when the exact knowledge of the variables and parameters is possible. In order to achieve this, all variables should be known without an error in magnitude and without a delay, all the parameters' values should be exactly correct, and there should not be a time difference between the desired control force and the actual control force applied. Existence of any of the mentioned deviations would cause the optimal heuristic to deteriorate in behavior,

quickly and vastly. The comparison of the behaviors generated by the heuristics in the presence of such errors is given in the next sections.

The duration of the landing in comparison to the bang-bang heuristic is slightly longer in the new heuristic and the terminal guidance heuristic. However, they are not as sensitive to the values of the parameters and variables and to minor actuator delays. Compared to the mass-spring-damper heuristic, they are not as robust to an error in parameter estimation, errors in variable readings, and the presence of an actuator delay. Nevertheless, they land the vehicle in significantly less time (see Table 8.1).

8.1. An Estimation Error in one of the Parameters

To be able to compare the deterioration in the results, we assumed that the value of *Mass* used in the heuristics is wrongly estimated. Four different types of mass estimation errors are used to compare the behaviors of the heuristics. Two of these estimation errors are absolute errors and the other two estimation errors are relative errors. In absolute errors, the deviation from the real value of the parameter is constant, and in relative errors the error is a percentage of the real value of the parameter. In this case, as the value of the parameter is constant, the difference between the relative error and absolute error is insignificant. This categorization of errors will be qualitatively different in the next sections. Therefore, this differentiation is made in this section, as well. First, as absolute errors, *Mass* is estimated as 950 kg and 1050 kg instead of 1000 kg, which are addressed as -50 kg and $+50$ kg, respectively. Second, the relative errors are defined as -10% and $+10\%$, which are equivalent to absolute errors of -100 kg and $+100$ kg, in this case.

The dynamic behavior generated by the heuristics in the presence of the -50 kg error is given in Figures 8.2, 8.3, 8.4, and 8.5. The *Landing Velocity* values for the mass-spring-damper, bang-bang, new heuristics and the terminal guidance heuristic deteriorate to -2.21 m/s, -25.59 m/s, -2.11 m/s, and -2.12 m/s; and the corresponding *Maximum Landing Force* values are 15,146 N, 93,466 N, 14,938 N, and 14,951 N; respectively. These values suggest that, in the case of a parameter estimation error, a great deterioration in the bang-

bang heuristic occurs, whereas the rest of the heuristics succeed in making a reasonable landing.

A summary with the important performance criteria of the landing is given in Table 8.2. An underestimation of *Mass* shortens *Landing Time* and causes an increase in *Landing Velocity*. The change in *Landing Velocity* in the bang-bang heuristic is significant and causes a crash, as expected. An overestimation of *Mass* lengthens *Landing Time* and reduces *Landing Velocity*, in the bang-bang heuristic as well. The other heuristics manage to tolerate these estimation errors.

Table 8.2. Comparison of the landing performances of the heuristics in the existence of an error in the parameter estimate *Mass*.

		Estimation Error in <i>Mass</i>			
		-50 kg	50 kg	-10%	10%
MSD	Landing Time (s)	53.01	57.76	50.44	59.93
	Landing Velocity (m/s)	-2.21	-1.92	-2.45	-1.83
Bang-Bang	Landing Time (s)	15.75	16.84	15.38	16.97
	Landing Velocity (m/s)	-25.59	-2.00	-36.14	-2.02
New	Landing Time (s)	22.16	22.93	21.77	23.30
	Landing Velocity (m/s)	-2.11	-1.86	-2.29	-1.75
Terminal Guidance	Landing Time (s)	21.45	22.27	21.03	22.67
	Landing Velocity (m/s)	-2.12	-1.98	-2.17	-2.00

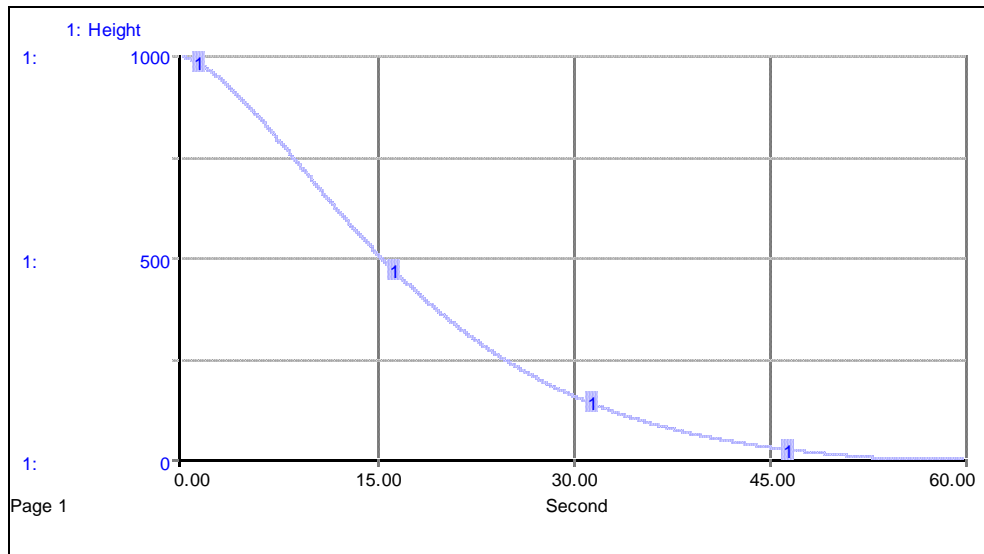


Figure 8.2. Landing behavior generated by the MSD heuristic in the presence of -50 kg error in the *Mass* estimate.

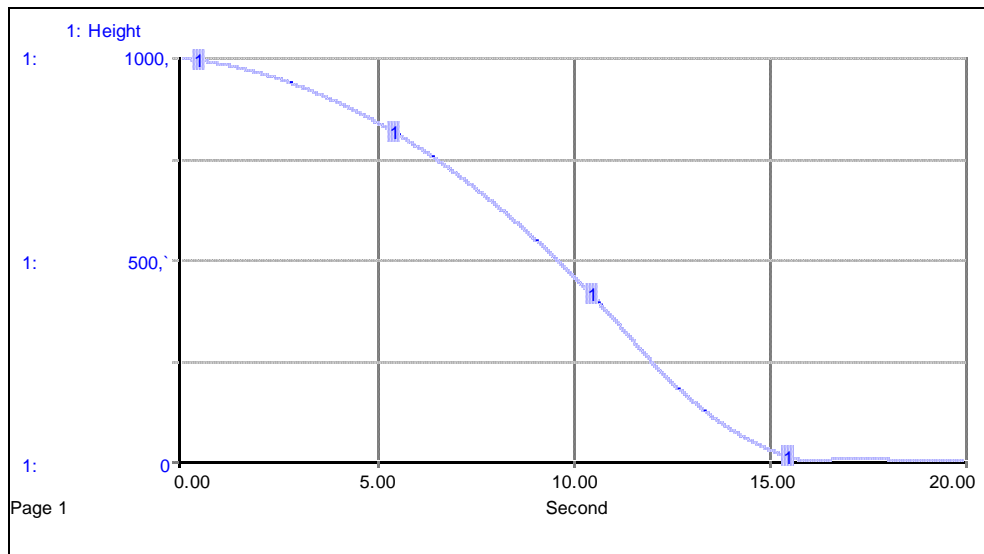


Figure 8.3. Landing behavior generated by the bang-bang heuristic in the presence of -50 kg error in the *Mass* estimate.

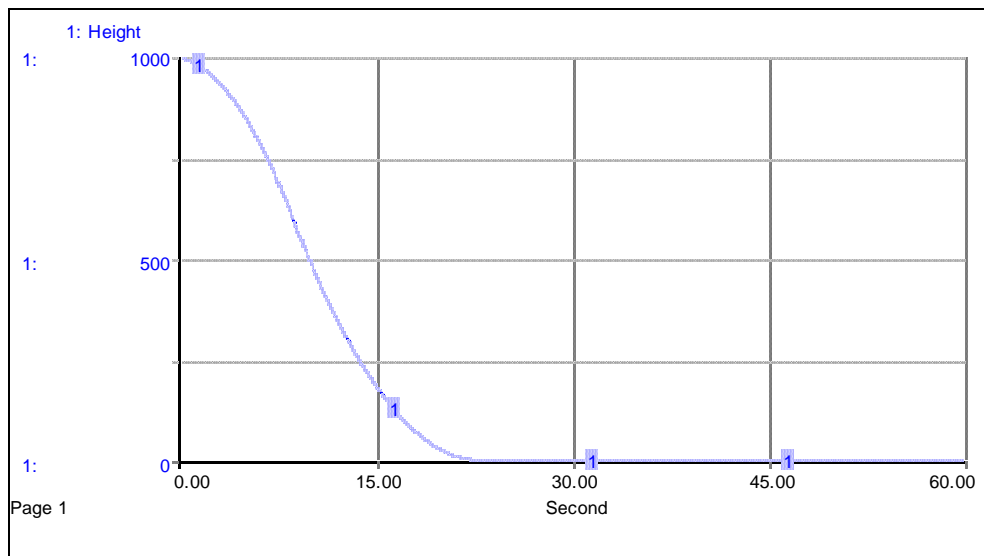


Figure 8.4. Landing behavior generated by the new heuristic in the presence of -50 kg error in the *Mass* estimate.

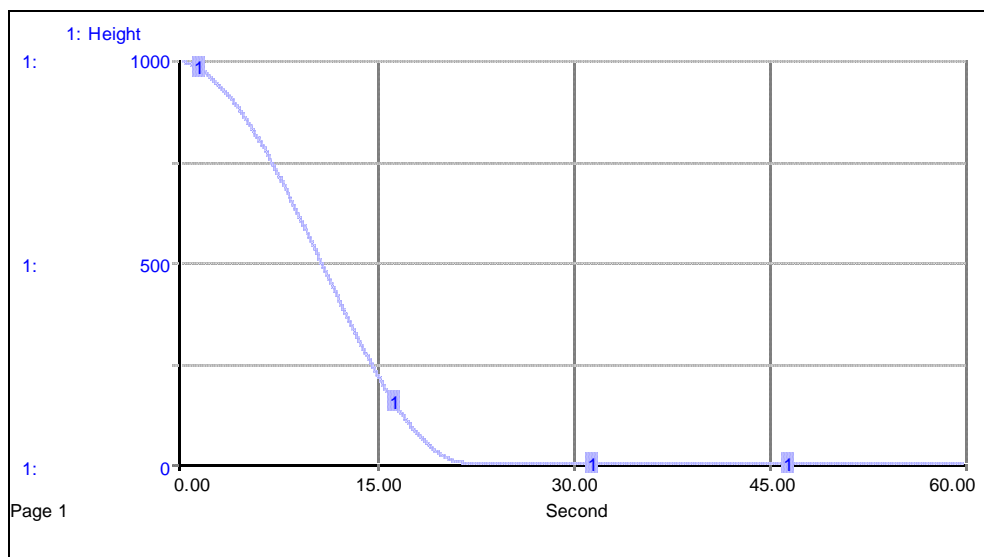


Figure 8.5. Landing behavior generated by the terminal guidance heuristic in the presence of -50 kg error in the *Mass* estimate.

8.2. An Error in Height Readings

We assumed that there is an error in *Height* readings; four different types of height estimation errors are used to compare the behavioral differences of the heuristics. Two of these errors are in absolute terms, meaning that the reading is off by a constant value throughout the landing. The other two are in relative terms, so that the read value is a constant percentage of the current value at any time. This time, the relative error and the absolute error are qualitatively different as the variable *Height* is changing during landing and the amount of the relative error changes with it. The absolute errors are -10 m and $+10$ m and the relative errors are -10% and $+10\%$ in this case. For $+10$ m error, *Height* is read by the heuristic 10 meters more than it is at all times during the simulation. The dynamic behavior generated by the heuristics in the presence of this error is given in Figures 8.6, 8.7, 8.8, and 8.9. The *Landing Velocity* values for the mass-spring-damper, bang-bang, new heuristics and the terminal guidance heuristic deteriorate to -2.86 m/s, -20.76 m/s, -11.36 m/s, and -14.46 m/s; and the corresponding *Maximum Landing Force* values are 16,721 N, 76,642 N, 44,296 N, and 54,890 N; respectively. Similar to the case with an error in the parameter estimates, the behavior generated by the bang-bang heuristic deteriorates more than the others. The new heuristic and the terminal guidance heuristic deteriorate as well, while mass-spring-damper heuristic makes a reasonable landing.

In the existence of a negative absolute error new heuristic and bang-bang heuristic do not succeed in making a landing. They hover a distance away from the ground as the erroneous *Height* value they consider is very close to zero. It can be seen from Table 8.3 that the cases with a positive relative error are managed well by all heuristics except for the bang-bang heuristic. All heuristics make a reasonable landing in the existence of a negative relative error, as the error gives the heuristics more space than they consider is available.

Table 8.3. Comparison of the landing performances of the heuristics in the existence of an error in the variable reading *Height*.

		<i>Height Reading Error</i>			
		-10 m	10 m	-10%	10%
MSD	Landing Time (s)	61.63	51.46	62.85	49.02
	Landing Velocity (m/s)	-1.21	-2.86	-1.81	-2.41
Bang-Bang	Landing Time (s)	no landing	15.92	17.00	15.44
	Landing Velocity (m/s)	no landing	-20.76	-2.02	-34.41
New	Landing Time (s)	no landing	21.24	32.86	30.28
	Landing Velocity (m/s)	no landing	-11.36	-1.86	-2.11
Terminal Guidance	Landing Time (s)	27.04	20.83	22.75	21.11
	Landing Velocity (m/s)	-1.89	-14.46	-2.00	-2.15

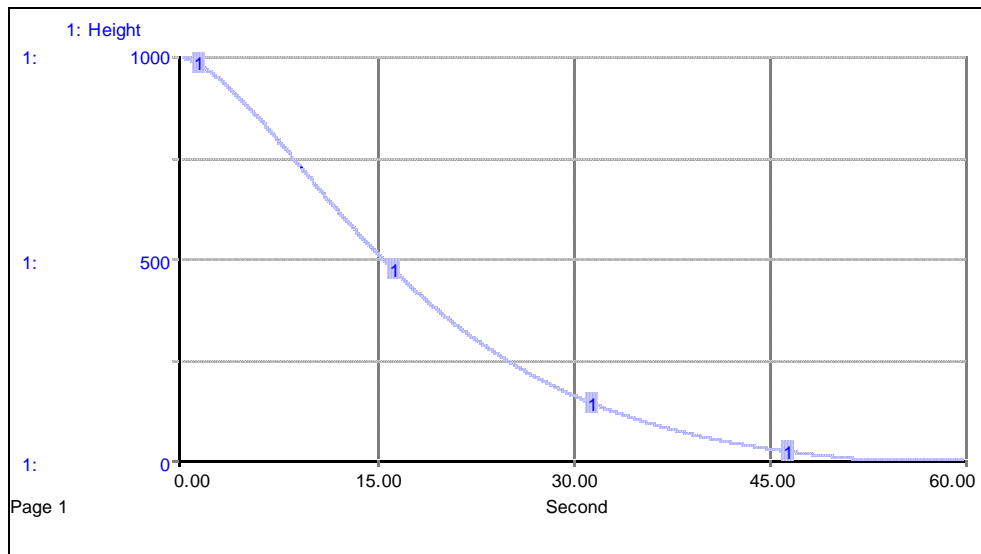


Figure 8.6. Landing behavior generated by the MSD heuristic in the presence of +10 m error in *Height* reading.

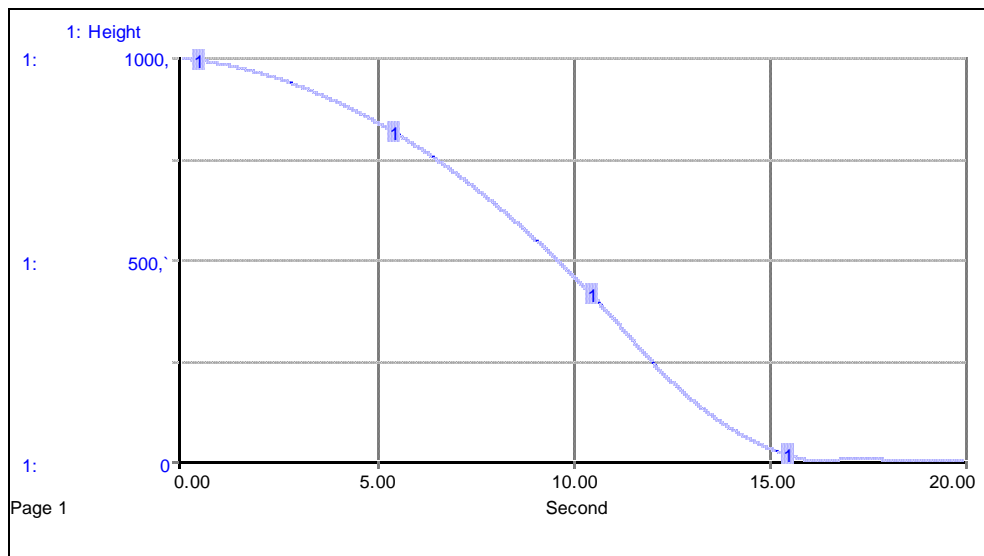


Figure 8.7. Landing behavior generated by the bang-bang heuristic in the presence of +10 m error in *Height* reading.

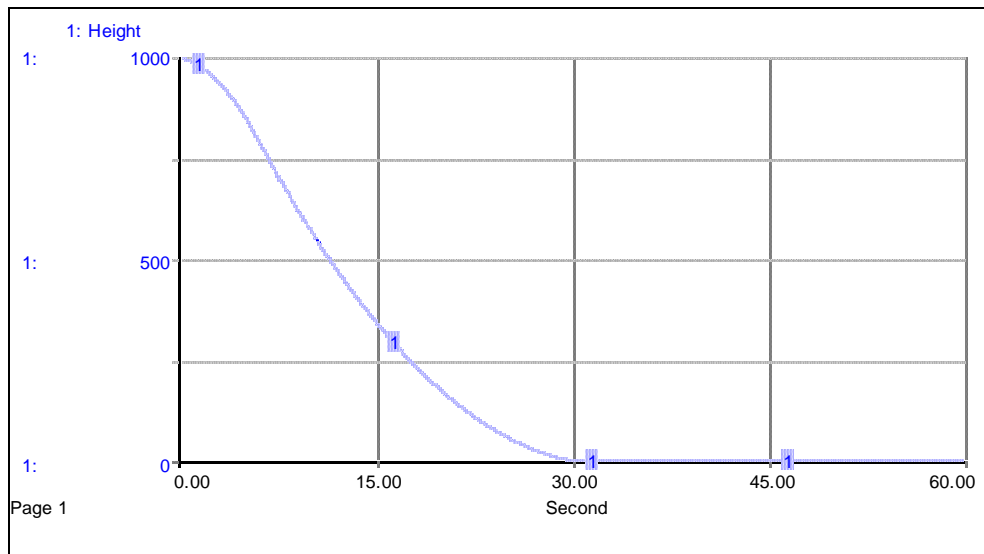


Figure 8.8. Landing behavior generated by the new heuristic in the presence of +10 m error in *Height* reading.

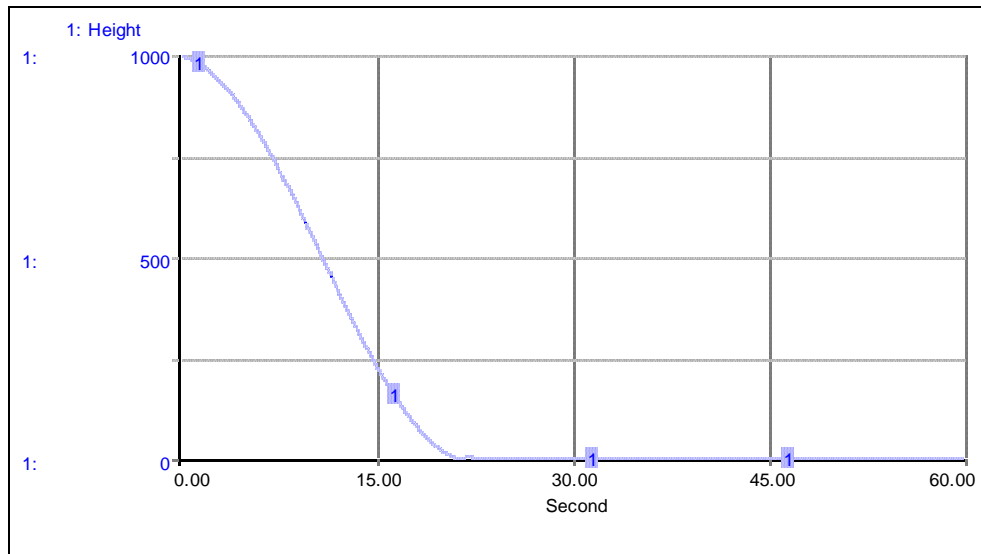


Figure 8.9. Landing behavior generated by the terminal guidance heuristic in the presence of +10 m error in *Height* reading.

8.3. The Presence of an Actuator Delay

In this section, we assume that there is an overlooked factor present in the model, an actuator delay (i.e. a delay in changing the level of the force created by the reverse force thruster). In this case, actuator delay is the time difference between the force that a heuristic demands and the application of that force. The behavior of the delayed output is affected by the duration and the order of delay. The resulting behaviors of same duration (2 seconds), but different orders of delay are given in Figure 8.10. The input is assumed to be 10, a constant. Outputs of different orders of delay are all assumed to be equal to zero, initially. Note that, discrete delay is also known as infinite order delay. It can be seen from the figure that smaller orders react more quickly to the discrepancy, but it takes more time for them to compensate for the whole difference.

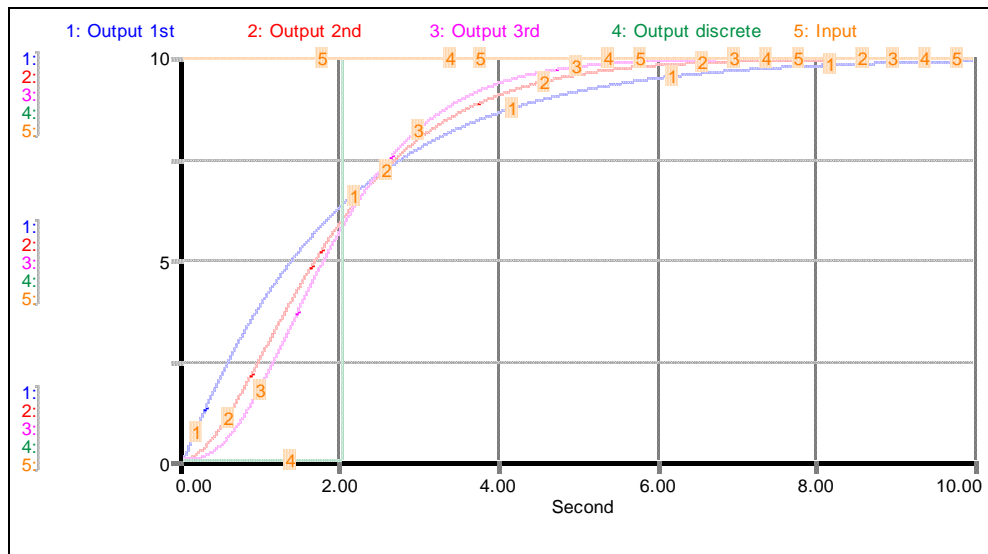


Figure 8.10. Responses of different order delay structures to a step input.

All four heuristics are evaluated with first order, second order, third order, and discrete (infinite order) actuator delays, where the duration of delay is 2 seconds in all cases. The landing performances of the heuristics with the inclusion of the four different orders of actuator delay can be seen in Table 8.4. Also the dynamic behaviors of landing in the presence of a discrete delay for different heuristics are given in Figures 8.11-8.14.

Table 8.4. Comparison of the landing performances of the heuristics in the existence of a 2 second actuator delay.

		Actuator Delay			
		1st order	2nd order	3rd order	discrete
MSD	Landing Time (s)	55.41	55.47	55.48	55.52
	Landing Velocity (m/s)	-1.74	-1.75	-1.75	-1.75
Bang-Bang	Landing Time (s)	14.20	14.10	14.06	13.96
	Landing Velocity (m/s)	-99.71	-107.09	-110.42	-120.48
New	Landing Time (s)	22.51	27.23	20.04	19.98
	Landing Velocity (m/s)	-1.94	-20.96	-21.59	-40.62
Terminal Guidance	Landing Time (s)	24.02	24.02	23.97	23.71
	Landing Velocity (m/s)	-6.94	-10.75	-12.81	-17.94

The presence of delay creates no significant change in the behavior generated by the mass-spring-damper heuristic (Figure 8.11) and the new *Landing Velocity* value generated by this heuristic is around -1.75 m/s for all orders of delay. However, a huge deterioration in the behavior generated by the bang-bang heuristic is observed. The new *Landing Velocity* values generated by this heuristic are between circa -100 m/s in the best case and -120 m/s in the worst case. The control applied by the bang-bang heuristic in the presence of an actuator delay is minimal. As a result, the *Landing Velocity* values generated by the bang-bang heuristic in the presence of a 2-second actuator delay are very close to the worst achievable *Landing Velocity* value that is -133.59 m/s. The worst achievable value is obtained by applying no control for the given initial conditions. New heuristic manages to make a reasonable landing in the presence of a first order delay, but fails to do so in the presence of higher order delays. This is due to the fact that, as the delay order increases, the instability of oscillations around *Desired Velocity* increases (see Figure 8.15).

Generally, when control becomes insufficient, *Landing Velocity* increases whereas *Landing Time* decreases, because of the early crash. A relatively big increase occurs in comparing *Landing Velocity* values of the first order delayed case to the second order delayed case of the new heuristic (Figure 8.16). The terminal guidance heuristic is able to make a hard landing with a first order delay and in the higher orders the *Landing Velocity* values increase to mild crashes.

Similar to the cases with an error in the parameter estimates and with an error in readings, mass-spring-damper heuristic manages a safe landing, proving its superiority in robustness as compared to the other heuristic.

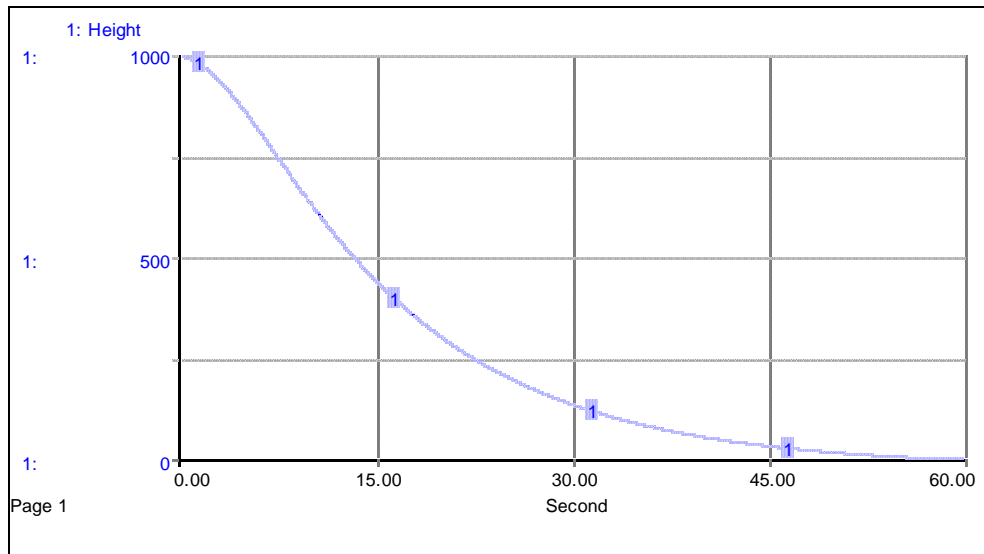


Figure 8.11. Landing behavior generated by the MSD heuristic in the presence of discrete actuator delay.

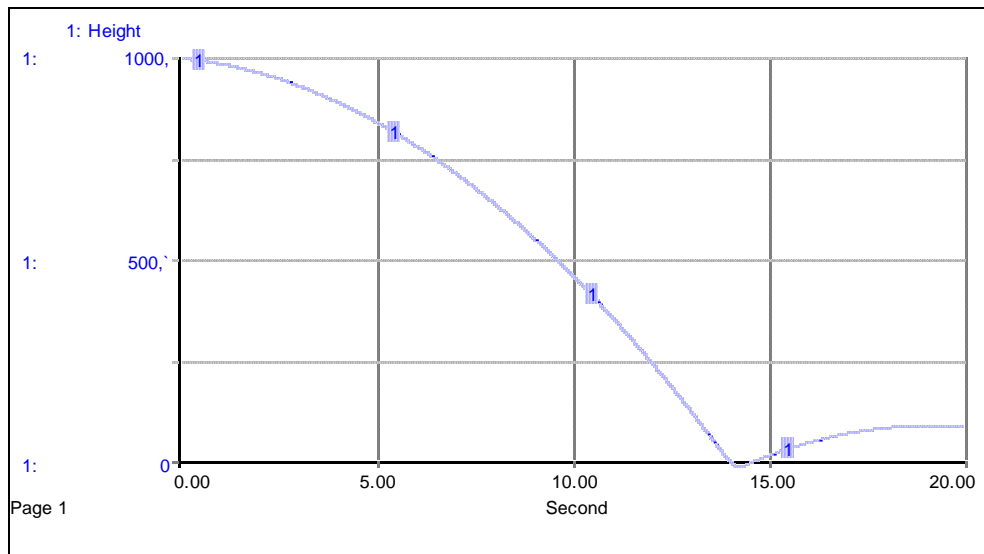


Figure 8.12. Landing behavior generated by the bang-bang heuristic in the presence of discrete actuator delay.

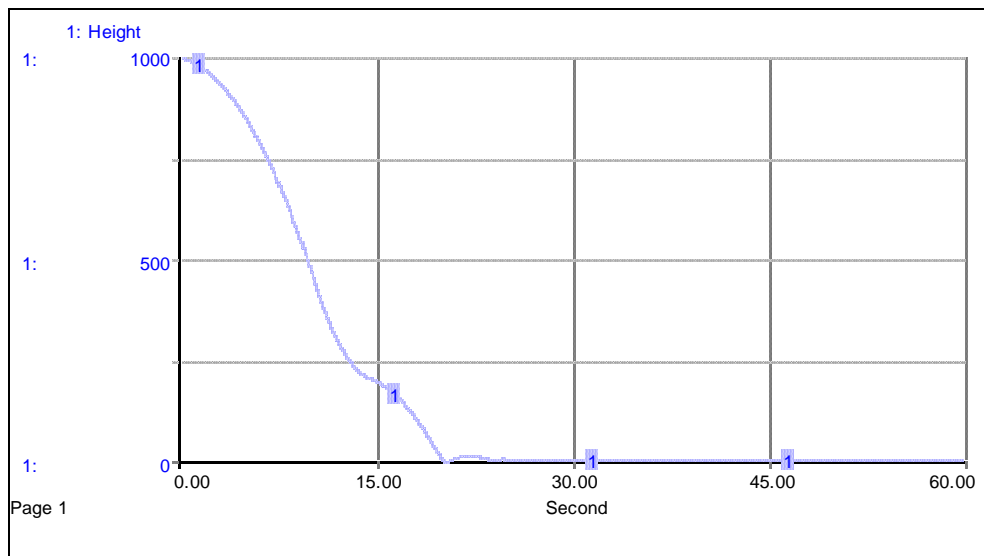


Figure 8.13. Landing behavior generated by the new heuristic in the presence of discrete actuator delay.

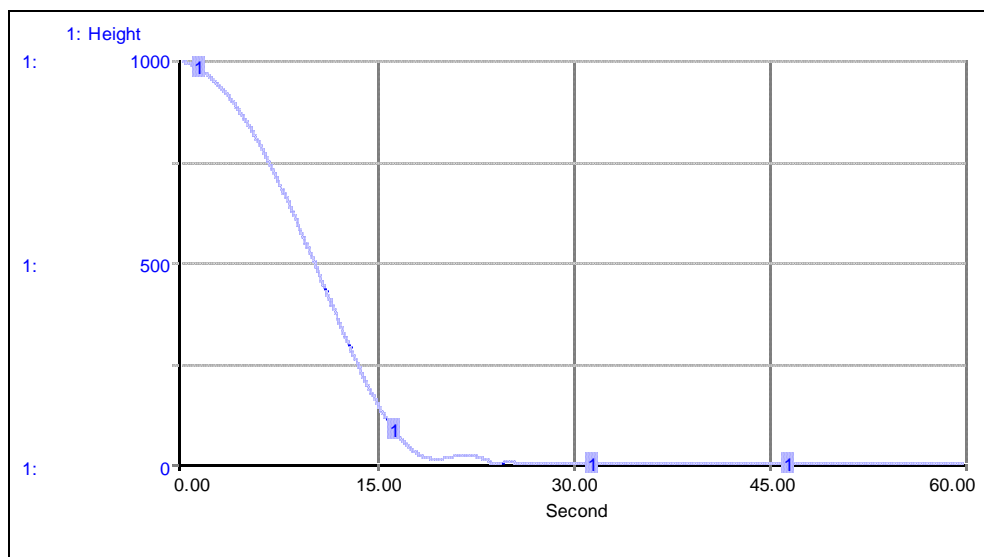


Figure 8.14. Landing behavior generated by the terminal guidance heuristic in the presence of discrete actuator delay.

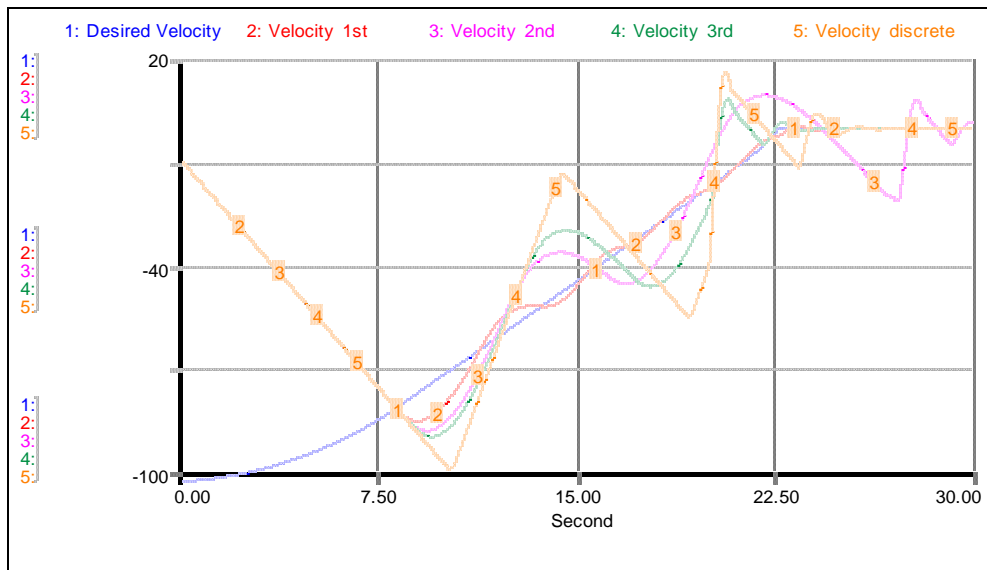


Figure 8.15. Velocity profiles of the new heuristic with different orders of delay.

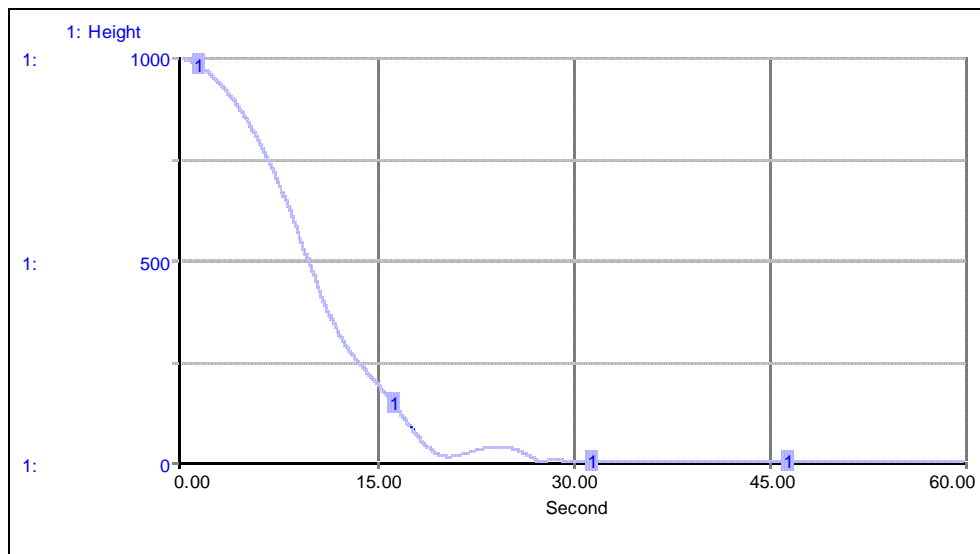


Figure 8.16. Landing behavior generated by the new heuristic in the presence of a second order delay of 2 seconds.

9. FUEL CONSUMPTION AND VARIABLE MASS

In previous chapters, it was assumed that the mass of the vehicle stays constant during landing. In real cases, when spacecrafts exert force they decrease in mass as they consume fuel for propulsion. With the inclusion of a decreasing predetermined amount of fuel it will also be possible to compare the heuristics' fuel consumptions.

This change in assumptions requires a modification to the previously explained soft landing model. The variable *Mass*, which was a constant before, is parted into two. It is comprised of the constant *Vehicle Mass* and the decaying *Fuel Mass*. In order to achieve this, *Fuel Mass* is a stock variable with a single outflow. This outflow will depend on *Control Force* and will be calculated based on a constant specific impulse. Specific impulse is a performance parameter describing the engine efficiency. The mass outflow from the engine is calculated based on the value of the specific impulse and the exerted force during landing. An engine with a higher specific impulse would exert more thrust with the same amount of fuel consumed (Huzel and Huang, 1992).

The equation for Mass instead of Equation 3.6 becomes:

$$Mass = Vehicle\ Mass + Fuel\ Mass \quad [kg] \quad (9.1)$$

$$Fuel\ Mass_{t+DT} = Fuel\ Mass_t + Change\ in\ Fuel\ Mass_t \cdot DT \quad [kg] \quad (9.2)$$

Generally, specific impulse is given as:

$$I_{sp} = \frac{F}{\dot{m} \cdot g_0} \quad [s] \quad (9.3)$$

or,

$$\dot{m} = \frac{F}{I_{sp} \cdot g_0} \quad [kg/s] \quad (9.4)$$

In these equations; F is the exerted force, I_{sp} is the specific impulse, g_0 is the gravitational acceleration constant 9.815 m/s^2 and \dot{m} is the momentary change in mass. For *Specific Impulse*, the real value from the rocket of the Apollo Lunar Module was taken. The outflow of the stock variable *Fuel Mass* becomes:

$$\text{Change in Fuel Mass} = -\frac{\text{Control Force}}{\text{Specific Impulse} \cdot g_0} \quad [\text{kg/s}] \quad (9.5)$$

$$\text{Specific Impulse} = 311 \quad [\text{s}] \quad (9.6)$$

$$g_0 = 9.815 \quad [\text{m/s}^2] \quad (9.7)$$

The initial value of *Fuel Mass* is taken to be sufficient under the condition that the *Max Force* is applied for 30 seconds. This amounts to an initial *Fuel Mass* of 300 kg. *Vehicle Mass* is taken as 700 kg so that the initial *Total Mass* is the same with the constant mass cases (i.e. cases without variable mass assumption).

$$\text{Fuel Mass}_0 = 300 \quad [\text{kg}] \quad (9.8)$$

$$\text{Vehicle Mass} = 700 \quad [\text{kg}] \quad (9.9)$$

The models with variable mass enable a comparison for the heuristics' fuel consumption to be made. The amount of fuel consumption is a better representation of the efficiency of the heuristics than *Landing Time*.

10. COMPARISON OF THE HEURISTICS UNDER VARIABLE MASS ASSUMPTION

Each one of the four heuristics with all of the errors and deviations explained in Chapter 8 has been simulated again under the variable mass assumption. The landing performances of the heuristics under the variable mass assumptions given in Table 10.1. Fundamentally, there is no behavioral difference between the landing performances of the runs under constant and variable mass assumptions.

Mostly, *Landing Time* values of the models with variable mass are less than their constant mass counterparts; an exception to this is the delayed versions of the mass-spring-damper (MSD) heuristic. This exception can be explained by the delayed reduction in *Control Force* for the mass-spring-damper heuristic before landing. Another exception to the main observation about the decrease in *Landing Time* is obtained by the bang-bang heuristic in the underestimated *Mass* case. As *Fuel Mass* is consumed, *Control Force* becomes more effective and bang-bang heuristic makes a more reasonable landing, decreasing *Landing Velocity* and increasing *Landing Time*.

The bang-bang heuristic's force utilization qualitatively changes with variable mass assumption. Under constant mass assumption, once the thruster is initiated, the bang-bang heuristic uses the thruster at its maximum force until touchdown. When mass decays in the form of fuel consumption, there is a need for the bang-bang heuristic to switch on and off the thruster for many times until touchdown. This different force utilizations are compared in Figure 10.1. *Net Force* is generated under constant mass assumption and *Net Force 2* is generated under variable mass assumption. It is worth mentioning that the maximum *Net Force* increases as time passes due to the decrease in mass, and, thus, decrease in *Gravitational Force*.

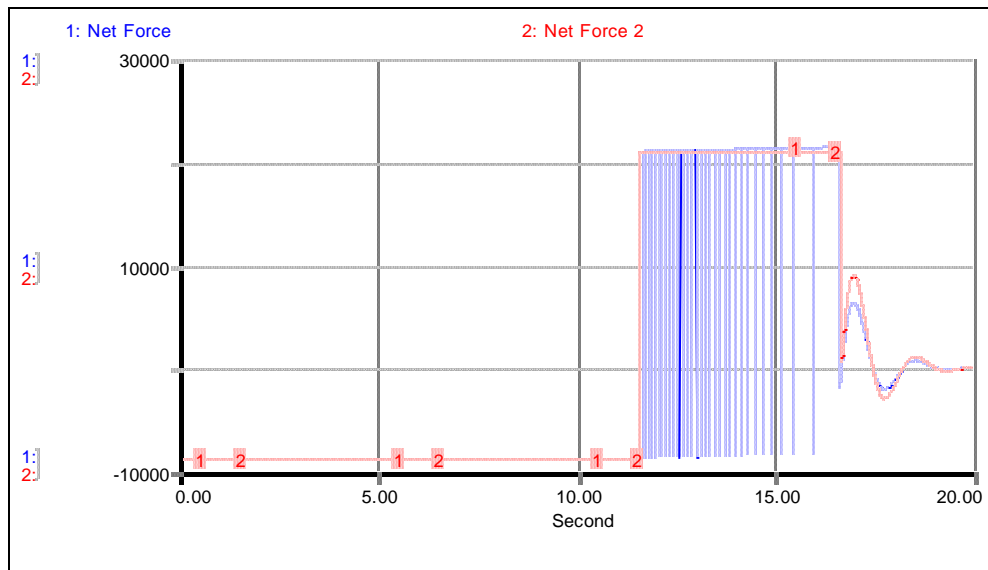


Figure 10.1. Force utilization of the bang-bang heuristic when mass decays due to fuel consumption.

Fuel consumption is the least in the bang-bang heuristic, as expected. New heuristic and terminal guidance heuristic consume similar amounts of fuel, even in the cases where they fail to achieve a reasonable landing; the only exception to this is the case with second-order delay, where the difference in the fuel consumption of the two exceeds 10 kg.

Mass-spring-damper heuristic takes two to three times the fuel the other heuristics take; disregarding the crash cases of the bang-bang heuristic, where there is almost no control and, thus, a very small amount of fuel consumption. Consequently, if the *Fuel Mass* were to be somewhat constrained, mass-spring-damper heuristic would be the first to be affected. It can also be said that an overestimation of *Mass* increases fuel consumption, while an underestimation of *Mass* decreases it.

Table 10.1. Comparison of the landing performances of the heuristics with variable mass.

		baserun	Estimation Error in Mass				Height Reading Error				Actuator Delay			
			-50 kg	50 kg	-10%	10%	-10 m	10 m	-10%	10%	1st	2nd	3rd	discrete
MSD	Landing Time (s)	54.72	52.22	57.07	49.94	58.95	61.16	50.71	61.76	48.79	57.94	57.96	57.97	57.98
	Landing Velocity (m/s)	-2.01	-2.19	-1.88	-2.40	-1.81	-1.12	-2.87	-21.79	-2.36	-1.37	-1.37	-1.38	-1.38
	Fuel Consumption (kg)	149.20	143.00	155.10	137.20	159.70	165.20	139.00	166.5	134.40	160.50	161.00	161.30	162.40
Bang-Bang	Landing Time (s)	16.61	15.91	16.75	15.45	16.87	none	15.86	-16.90	15.52	14.20	14.10	14.06	13.96
	Landing Velocity (m/s)	-2.38	-19.28	-2.01	-32.44	-2.01	none	-21.31	2.01	-30.42	-99.46	-106.94	-110.30	-120.45
	Fuel Consumption (kg)	49.50	42.30	50.00	36.90	50.30	59.80 ⁸	41.50	-50.40	37.70	25.60	25.30	25.00	24.00
New	Landing Time (s)	22.22	21.84	22.59	21.47	22.94	none	20.98	22.97	21.58	22.26	27.79	19.96	19.98
	Landing Velocity (m/s)	-2.09	-2.28	-1.97	-2.43	-1.87	none	-11.85	-1.98	-2.23	-1.23	-23.10	-22.47	-42.38
	Fuel Consumption (kg)	65.00	63.90	66.00	62.80	67.00	86.50 ⁸	58.60	67.00	63.20	73.30	83.10	71.10	66.00
Terminal Guidance	Landing Time (s)	21.86	21.44	22.28	21.03	22.67	27.04	20.83	22.75	21.11	23.61	23.61	23.57	23.30
	Landing Velocity (m/s)	-2.03	-2.10	-1.98	-2.12	-2.00	-1.98	-14.46	-2.00	-2.11	-5.61	-9.20	-11.22	-16.64
	Fuel Consumption (kg)	64.00	62.80	65.10	61.70	66.20	79.10	57.40	66.40	61.90	71.50	70.50	70.20	69.60

⁸ In these cases, the vehicle does not land during the simulation run. Therefore, the values obtained are affected by the length of the simulation.

11. CONCLUSION

In this thesis, we study the soft landing of a vehicle on a surface in the absence of atmospheric molecules and we assume the landing process is controlled only by a reverse force thruster. The focus of the study is only on the movement in the vertical axis. Therefore, we ignore the movement of the spacecraft in the horizontal axes. We first build a soft landing model under these main assumptions. The model and the modeling process is discussed in full detail including the analyses for parameter value selection. Later, we derive three heuristics for the control of the soft landing model; the mass-spring-damper heuristic, the bang-bang heuristic, and a new heuristic, which is a combination of the first two. As a fourth heuristic, the terminal guidance heuristic is adapted from the work of Kriegsman and Reiss (1962). We disclose the entire derivation process for and discuss the behaviors obtained by the four heuristics. We tested the performances of these heuristics in the presence of an error in the parameter estimates; in the presence of an error in the height readings; and in the presence of an overlooked factor such as a delay in changing the level of the force created by the reverse force thruster, which is known as actuator delay.

The mass-spring-damper based control heuristic requires a longer landing time compared to the other two heuristics, but it is more robust compared to the bang-bang control heuristic in the sense that it is less sensitive to the errors in parameter values, errors in readings, and presence of an actuator delay. Note that even in the absence of errors and delays, mass-spring-damper heuristic may crash the spacecraft depending on the initial conditions, which is intolerable. Bang-bang heuristic minimizes the time needed to land under the assumed conditions. However, this aggressive management of the time needed to land may make it crash the spacecraft under realistic conditions (e.g. a small deviation from assumed conditions).

The new heuristic is developed by including the weight of supply line concept from the system dynamics literature, and combining the mass-spring-damper based heuristic and the bang-bang heuristic. The new heuristic is not superior to the mass-spring-damper heuristic and the bang-bang heuristic regarding all performance criteria. However, it is exempt from the intolerable weaknesses of the both (i.e. high dependency on initial

conditions of the mass-spring-damper heuristic and the high sensitivity to errors and delays of the bang-bang heuristic).

An overestimation of *Mass* causes no problems for any of the heuristics, including the bang-bang heuristic; whereas an underestimation of *Mass* causes the bang-bang heuristic to crash.

Absolute errors in *Height* readings are problematic in all heuristics except mass-spring-damper heuristic. An absolute underestimation of *Height* causes the bang-bang heuristic and the new heuristic not to land, the terminal guidance heuristic makes a reasonable landing. An absolute overestimation of *Height*, however, causes the three heuristics except mass-spring-damper heuristic to crash. Relative errors in *Height* reading are not problematic for the heuristics except for the relative overestimation case in the bang-bang heuristic.

The presence of an actuator delay causes no problems for the mass-spring-damper heuristic and the new heuristic is able to handle first-order delay. Generally, with higher orders of delay, the landing gets more problematic. The behavior resulting from the bang-bang heuristic is very poor; the landing performance is almost like the case where no control is applied at all. The new heuristic and the terminal guidance heuristic attain positive velocities during simulation, which means they show undesired oscillatory behavior.

The deteriorations observed in the cases under variable mass assumption are similar to the deteriorations observed in the cases with constant mass assumption; there is no qualitative difference between the behaviors obtained under both assumptions, *ceteris paribus*. Generally, *Landing Time* values of the models with variable mass are less than their constant mass counterparts; an exception to this is the delayed versions of the mass-spring-damper heuristic. This exception can be explained by the delayed reduction in *Control Force* for the mass-spring-damper heuristic before landing.

Fuel consumption is the least in bang-bang heuristic, as expected. New heuristic and terminal guidance heuristic consume similar amounts of fuel, even in the cases where they

fail to achieve a reasonable landing; the only exception to this is the case with second-order delay, where the difference in the fuel consumption of the two exceeds 10 kg. Mass-spring-damper heuristic takes two to three times the fuel the other heuristics take; disregarding the crash cases of the bang-bang heuristic, where there is almost no control and, thus, low fuel consumption. Consequently, if *Fuel Mass* were to be somewhat constrained, mass-spring-damper heuristic would be the first to be affected. It can also be said that an overestimation of *Mass* increases fuel consumption, while an underestimation of *Mass* decreases it.

The main performance criteria are *Landing Time*, *Landing Velocity*, whether or not the operating range is limited, and robustness. According to this study, none of the heuristics presented in this thesis satisfy all the performance criteria. A heuristic that is the best according to one criterion may be the worst in the other. Hence, none of the heuristics is superior to the rest in all aspects.

The mass-spring-damper heuristic is robust in the sense that it is the least sensitive to the deviations from the model assumptions. However, *Landing Time* for this heuristic is the longest, which also results in high fuel consumption. Moreover, this heuristic has a limited operating range; it crashes the vehicle if the initial conditions are outside of the operating range.

The bang-bang heuristic gives the shortest landing time, but it is not robust in the sense that it is sensitive to all types of deviations from the model assumptions such as an error in the mass estimate, an error in the height reading, and the presence of an actuator delay. Even a minor deviation is highly risky for this heuristic.

The new heuristic introduced in this thesis aims to avoid the weaknesses of the mass-spring-damper and bang-bang heuristics. As a result, this heuristic gives a reasonable *Landing Time*, does not have a limited operating range, and it is less sensitive to the deviations from the model assumptions than the bang-bang heuristic. However, it does not outperform the mass-spring-damper and bang-bang heuristics in all performance criteria. Although, the formulations and the dynamic behaviors of the terminal guidance heuristic and the new heuristic are different, their landing performances are similar. Therefore, the

main conclusions about the new heuristic regarding the performance criteria are also valid for the terminal guidance heuristic.

According to this study, it is very difficult to find a control heuristic that satisfies all performance criteria even for a very basic model of soft landing. Especially, the existence of an actuator delay further complicates this control problem. As a future study, we are planning to improve the new heuristic and the terminal guidance heuristic so as to obtain a reasonable behavior at least in the presence of a minor actuator delay.

APPENDIX A: CALCULATION OF THE CRITICAL POINT IN THE BANG-BANG HEURISTIC

The kinetic energy available at the critical point should be cancelled by the work done by the resultant force.

$$E_{k1} = -\left(\frac{\text{Gravitational}}{\text{Force}}\right) \cdot \left(\left(\frac{\text{Initial}}{\text{Height}}\right) - \left(\frac{\text{Critical}}{\text{Height}}\right)\right) + \frac{\text{Mass}}{2} \cdot \left(\frac{\text{Initial}}{\text{Velocity}}\right)^2 [J] \quad (\text{A.1})$$

$$E_{k2} = \frac{\text{Mass}}{2} \cdot \left(\frac{\text{Desired Final}}{\text{Velocity}}\right)^2 [J] \quad (\text{A.2})$$

$$W = \left(\left(\frac{\text{Max}}{\text{Force}}\right) + \left(\frac{\text{Gravitational}}{\text{Force}}\right)\right) \cdot \left(\frac{\text{Critical}}{\text{Height}}\right) [J] \quad (\text{A.3})$$

$$W = \Delta E_k [J] \quad (\text{A.4})$$

Plugging in model parameters and initial conditions gives out a *Critical Height* of 297.27 meters.

REFERENCES

- Åström, K.J., and R.M. Murray, 2008, *Feedback Systems: An Introduction for Scientists and Engineers*, Princeton University Press, Princeton, NJ.
- Atay, F.M., 2009, *Complex Time-Delay Systems: Theory and Applications*, Springer, Berlin.
- Barlas, Y., 2002, “System Dynamics: Systemic Feedback Modeling for Policy Analysis”, In *Knowledge for Sustainable Development - An Insight into the Encyclopedia of Life Support Systems*, UNESCO/EOLSS Publishers, Paris, France; Oxford, UK, pp. 1131–1175.
- Barlas, Y., and M.G. Ozevin, 2004, “Analysis of Stock Management Gaming Experiments and Alternative Ordering Formulations”, *Systems Research and Behavioral Science*, Vol. 21, No. 4, pp. 439–470.
- Barlas, Y., and H. Yasarcan, 2006, “Goal Setting, Evaluation, Learning and Revision: A Dynamic Modeling Approach”, *Evaluation and Program Planning* Vol. 29, No. 1, pp. 79–87.
- Cantoni, V., S.F. Finzi, 1980, “Slowest Descent on the Moon”, *SIAM Review*, Vol. 22, No. 4, pp. 495–499.
- Fleming, W.H. and R.W. Rishel, 1975, *Deterministic and Stochastic Optimal Control*, Springer-Verlag.
- Forrester, J.W., 1961, *Industrial Dynamics*, Pegasus Communications, Waltham, MA.
- Forrester, J.W., 1971, *Principles of Systems*, Pegasus Communications, Waltham, MA.

- Herdem, C., and H. Yasarcan, 2010, “Dynamics of Glucose-Insulin Regulation: Insulin Injection Regime for Patients with Diabetes Type 1”, *Proceedings of The 28th International System Dynamics Conference*, Seoul - Korea.
- Huzel, D.K., and D.H. Huang, 1992, *Modern Engineering for Design of Liquid-Propellant Rocket Engines*, AIAA, Washington DC., pp. 12–19.
- Klumpp, A.R., 1974, “Apollo Lunar Descent Guidance”, *Automatica*, Vol. 10, pp. 133–146.
- Kriegsman, B.A., and M.H. Reiss, 1962, “Terminal Guidance and Control Techniques for Soft Lunar Landings”, *ARS Journal*, Vol. 32, pp. 401–413.
- LaSalle, J.P., 1959, “Time Optimal Control Systems”, *Proceedings of the National Academy of Sciences of the United States of America*, Vol. 45, No. 4, pp. 573–577.
- Liu, X.L., G.R. Duan, and K.L. Teo, 2008, “Optimal Soft Landing Control for Moon Lander”, *Automatica*, Vol. 44, No. 4, pp. 1097–1103.
- Maynard, H.B., 1971, *Industrial Engineering Handbook* (3rd edn), McGraw-Hill, New York.
- Meditch, J.S., 1964, “On the Problem of Optimal Thrust Programming for a Lunar Soft Landing”, *IEEE Transactions on Automatic Control*, Vol. 9, No. 4, pp. 477–484.
- Michiels, W., and S.I. Niculescu, 2007, *Stability and Stabilization of Time-Delay Systems: An Eigenvalue-Based Approach*, Society for Industrial and Applied Mathematics.
- Rosen, M.W., and F.C. Schwenk, 1959, “A Rocket for Manned Lunar Exploration”, *IRE Transactions on Space Electronics and Telemetry*, Vol. 4, pp. 155–162.

- Sterman, J.D., 1989, "Modeling Managerial Behavior: Misperceptions of Feedback in a Dynamic Decision Making Experiment", *Management Science*, Vol. 35, No. 3, pp. 321–339.
- Sterman, J.D., 2000, *Business Dynamics: Systems Thinking and Modeling for a Complex World*, Irwin/McGraw-Hill, Boston, MA.
- Wikipedia, *Apollo 15*, 2011, http://en.wikipedia.org/wiki/Apollo_15, 16 September 2011.
- Wu, K.C., J. Antol, J.J. Watson, R.J. Saucillo, D.D. North, and D.D. Mazanek, 2007, "Lunar Lander Structural Design Studies at NASA Langley." *AIAA SPACE*.
- Yasarcan, H., 2003, *Feedback, Delays and Non-Linearities in Decision Structures*, Ph.D. Thesis, Boğaziçi University.
- Yasarcan, H., 2010, "Improving Understanding, Learning, and Performances of Novices in Dynamic Managerial Simulation Games", *Complexity*, Vol. 15, No. 4, pp. 31–42.
- Yasarcan, H., 2011, "Stock Management in the Presence of Significant Measurement Delays", *System Dynamics Review*, Vol. 27, No. 1, pp. 91–109.
- Yasarcan, H., and Y. Barlas, 2005, "A Generalized Stock Control Formulation for Stock Management Problems Involving Composite Delays and Secondary Stocks", *System Dynamics Review*, Vol. 21, No. 1, pp. 33–68.
- Zhou, J., D. Zhou, K.L. Teo, G. Zhao, 2009, "Nonlinear Optimal Feedback Control for Lunar Module Soft Landing", *IEEE International Conference on Automation and Logistics*, pp. 681–685.